CHALMERS
UNIVERSITY OF TECHNOLOGY

Aalto-yliopisto
Aalto-universitetet
Aalto University

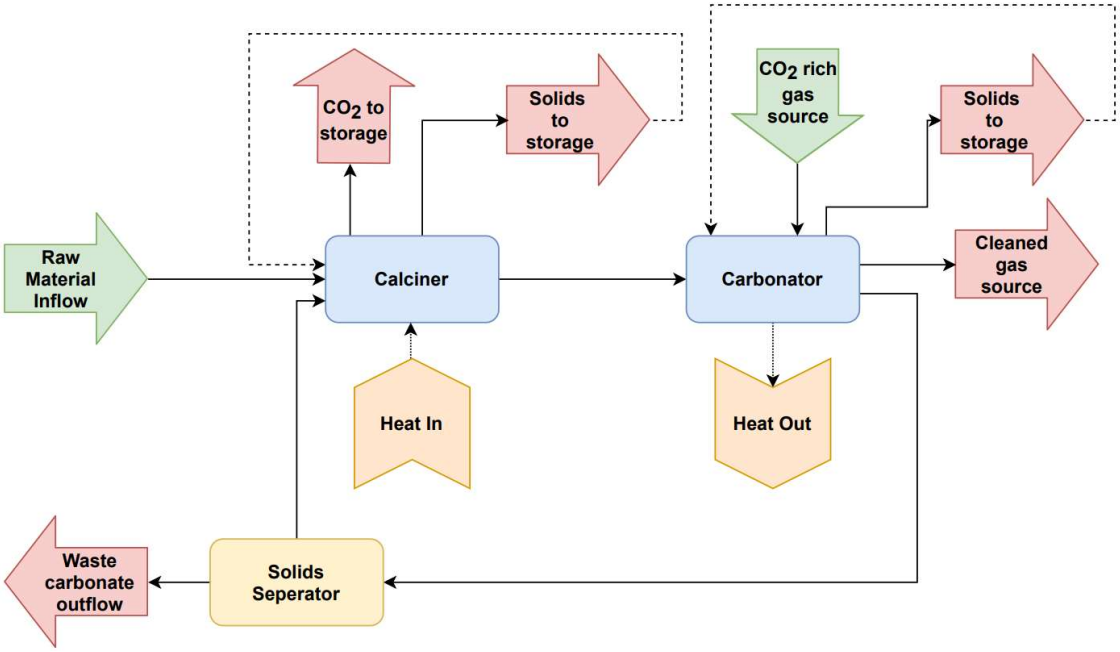

Techno-Economic Study of Solid Cycles for Thermochemical Energy Storage and Carbon Capture

Master's thesis in Sustainable Energy Engineering

Cameron Tinkler

DEPARTMENT OF SPACE, EARTH AND ENVIRONMENT
DIVISION OF ENERGY TECHNOLOGY

CHALMERS UNIVERSITY OF TECHNOLOGY
Gothenburg, Sweden 2021
www.chalmers.se

Table of Contents

Acknowledgement

I would like to thank my supervisors Carolina Guio-Perez and Guillermo Castilla for their continued support throughout the project. I appreciate the substantial time spent discussing the work and bringing new ideas to the table to shape the direction of the project. Also, I value the friendly nature and openness of our relationship, it certainly made the project a lot more enjoyable!

Secondly, I would like to thank my examiners David Pallares and Mika Jarvinen for their support over the course of the project, keeping meetings light-hearted and friendly throughout and always being approachable. The same goes to everyone in the fluidisation group here at Chalmer's, I found our fortnightly meetings insightful.

I would also like to thank Corey Blackman from SaltX Technology for his continued support throughout the project, helping to direct the work and maintain its vision.

Additionally, I would like to thank Stavros Papadokonstantakis for his assistance with the Aspen+ modelling.

Finally, I would like to thank my family for supporting me unconditionally throughout this project, my studies and life as a whole.

Abstract

A techno-economic analysis of the calcium looping cycle for combined thermochemical energy storage and carbon capture is presented within this work. A steady-state process model was developed using Aspen+ software, following the simulation of both an open-loop cycle with continual system clearing, and a closed-loop cycle with a different targeted number of particle cycles as well as different carbon capture rates. The model computes the mass and energy balances of the system under different conditions, which are consecutively used to evaluate the economic potential of the different cases studied. For the cases presented within this thesis, cycling the solid material 9 times prior to discharge provided the best economic results, with the most favourable NPV output over the plant lifetime, although the net energy conversion was lower (~16% reduction) than that of a system with 1 solids cycle prior to system discharge. The trend indicates that past a certain point - in this work Ncyc=3 - the NPV of the system rises with increasing particle cycle number. To maintain particle activity whilst increasing solids cycling number a continual make up flow is required, the purge and make-up flows increase in size with rising cycle number. The costs associated with these flows can be compared to the cost of clearing the system following a lesser number of cycles, demonstrating that increasing the number of solid-cycles within the system should eventually reduce the operational expenditure. A further sensitivity analysis was undertaken to determine the impact of varying carbon capture rates on the economic potential of the process. Of the studied cases a carbon capture rate of 0.95 presented the best economic results for a particle cycle number of 1, whilst a carbon capture rate of 0.9 proved more profitable for the higher particle cycle number of 9, given the economic assumptions made within the work. The trends presented within the carbon capture sensitivity analysis indicate the importance of the economic inputs, such as carbon tax and electricity prices, on determining the optimum capture rate, similarly indicating that the optimum capture rate will vary depending on the number of solids cycles the material undergoes. The variation in carbon capture rate presented within this work highlights the economic potential of solids storage (and hence energy storage) versus carbon tax profits, the model can be adjusted to develop further research determining optimum values for different cases

Glossary

Anacronym	Meaning
Aspen	Advanced System for Process Engineering Computer Software
$CaCO_3$	Calcium carbonate
CaL	Calcium looping
CAPEX	Capital Expenditure
CaO	Calcium oxide
CC	Carbon Capture
CCS	Carbon Capture Storage
CEPCI	Chemical Engineering Plant Cost Index
CFB	Circulating Fluidised Bed
CLC	Chemical Looping Combustion
CLR	Chemical Looping Reforming
CO_2	Carbon dioxide
CSP	Concentrating Solar Power
EES	Electrical Energy Storage
FG	Flue Gas
LHS	Latent Heat Storage
HX	Heat Exchanger
MOx	Metal oxide
NPV	Net Present Value
OPEX	Operational Expenditure
PCM	Phase Change Material
SHS	Sensible Heat Storage
TCES	Thermochemical Energy Storage
TES	Thermal Energy Storage
TRL	Technology Readiness Level
VRE	Variable Renewable Energy

Nomenclature	Definition
Clean Flue Gas	Flue gas with targeted CO_2 removed
Dependent Variable	Measurable output quantity which is a function of independent variables and parameters
Fluidisation Agent	Fluid providing velocity to solid particle bed within reactor to induce fluidisation
Bed Material	Inert solid material contained within fluidised bed reactors to facilitate enhanced heat transfer
Independent Variable	A quantity externally controlled and varied
Parameter	Quantity that is set/determined by model but not externally varied by user
Particle Cycle Number	Number of cycles solids undergo within the process prior to discharge
Test Case	Determines the effect of changing key variable within sensitivity analysis
Test Series	A group of test cases
Test Simulation	The variation of a set property for which all test cases are examined to provide a data range within each case

Variable	Meaning	Unit
C_{elec}	Cost of electricity	€/MWh_{el}
C_{steam}	Cost of steam	€/MWh_{th}
f_{calc}	Fraction of calcination of all particles within system	mol_{CaO}/mol_{tot}
f_{carb}	Fraction of carbonation of all particles within system	mol_{CaCO3}/mol_{tot}
F_0	Make up flow rate	mol/s
F_R	Solids recirculation flow rate	mol/s
Δh_{react}	Reaction enthalpy	kJ/mol
k	Deactivation constant	
$\dot{m}_{CaCO3}$	Calcium carbonate mass flow rate	kg/s
N	Number of carbonation cycles	
N_{cyc}	Particle cycle number	
$\eta_{calciner}$	Calciner efficiency	%
η_{steam}	Efficiency of steam cycle	%
$\dot{Q}_{input}$	Heat input	W
r_N	Fraction of particles carbonated N times within the cycle	$mol_{carb/cycle}/mol_{cycle}$
X_{calc}	Conversion to CaO of solids leaving the calciner	
X_{carb}	Conversion to $CaCO_3$ of solids leaving the carbonator	
X_{CO2}	Carbon capture rate	mol_{CO2out}/mol_{CO2in}
X_N	Carbonation Conversion	
X_r	Residual conversion of CaO following infinite cycling	

List of Figures

List of Tables

List of Equations

1. Introduction

1.1. Background

The commitment to constrain global temperature rise to a maximum of 2°C and preferably below 1.5°C above pre-industrial levels has motivated a globalised effort to decarbonise the energy system. [1] In order to achieve these goals increased integration of variable renewable energy (VRE) will prove essential, with energy storage technologies and low carbon dispatchable energy sources likely to play a key role this transition. [2]

Energy storage technologies are implemented when there is an excess of power produced compared to that required. The technologies store the energy for release at a period when there is a deficit of power required compared to that being produced. [3] A common example of this variation between production and demand would be an excess of solar power produced during daylight hours compared when demand is low, compared to reduced production of solar energy in the night hours whilst demand is maintained. [4]

Thermal and thermochemical energy storage (TCES) solutions for heat and power production have received research and investment, perceived as a means of providing services typical of energy storage systems including increased grid flexibility and improving the integration of VRE sources [5]. Among other reasons, TCES is gaining special attention due to its capability for high temperature discharge, high energetic and exergetic efficiencies when compared with sensible heat alternatives, and its potential for long term storage and transportability [6, 7]. The basis of all TCES technologies is relatively similar: providing thermal energy to power an endothermic reaction, storing the products and recombining them in an exothermic reaction to release heat. [8]

Carbon Capture Storage (CCS) technologies could play an integral part in the decarbonisation of numerous industries, with certain process designs reaching industrial maturity. However, currently the market is dominated by single purpose chemical absorption and physical separation technologies. [9] These technologies have not proved financially viable in many power markets, and as such the focus is increasingly directed towards cost reduction through process optimisation and investigation of alternative technology. [10]

The optimisation of material usage in both energy storage and carbon capture technologies is of growing interest as concerns rise over the availability and environmental impact of materials required. [11, 12] One method to reduce this impact is to seek technologies combining applications, capable of efficiently storing energy, whilst capturing carbon emissions. [13]

To achieve combined TCES-CCS applications studies have focussed upon carbonate-based precursor materials, which emit and absorb CO_2 in a reversible reaction. [6, 14, 15] For this reason, Calcium Looping (CaL) systems are of particular interest. CaL systems have been verified in pilot plants at up to MW_{th} scale for post combustion CO_2 capture [16], [17], [18], reaching a Technology Readiness Level (TRL) of 6-7 [19]. Pilot projects have also been demonstrated for TCES applications, primarily when integrated with Concentrated Solar Power (CSP) plants [20, 21], however, there has been limited research into its use for combined applications to date.

The CaL-TCES process typically follows the scheme presented in Figure 1. A carbonate precursor material circulates between two reactors, with storage potential between each

stage. During the calcination stage, high temperatures facilitate the thermal decomposition of the carbonate to form reaction products – including an oxide and CO_2 – as detailed in Eq. 1. The products can be stored separately before being recombined in the carbonator reactor to release thermal energy. [4]

$$Carbonate + \Delta h_{react} \leftrightarrow Oxide + CO_2 + biproduct \qquad (Eq. 1)$$

Precursor materials may vary, but most often the materials are a variation of limestone ($CaCO_3$) or dolomite ($CaMg(CO_3)_2$) dependent on cost and environmental impact. [8] The choice of precursor material (chemical make-up, purity etc.) impacts upon the required reaction conditions for cycling. [8]

Figure 1 details a system specifically focussed on energy storage, should the process aim to include CCS, the CO_2 should be separated following the calciner reactor, with an external source of CO_2 flowing into the carbonator reactor. A typical external CO_2 source would be flue gas (FG) from a thermal power plant or CO_2 emitted during cement production. [22, 23]

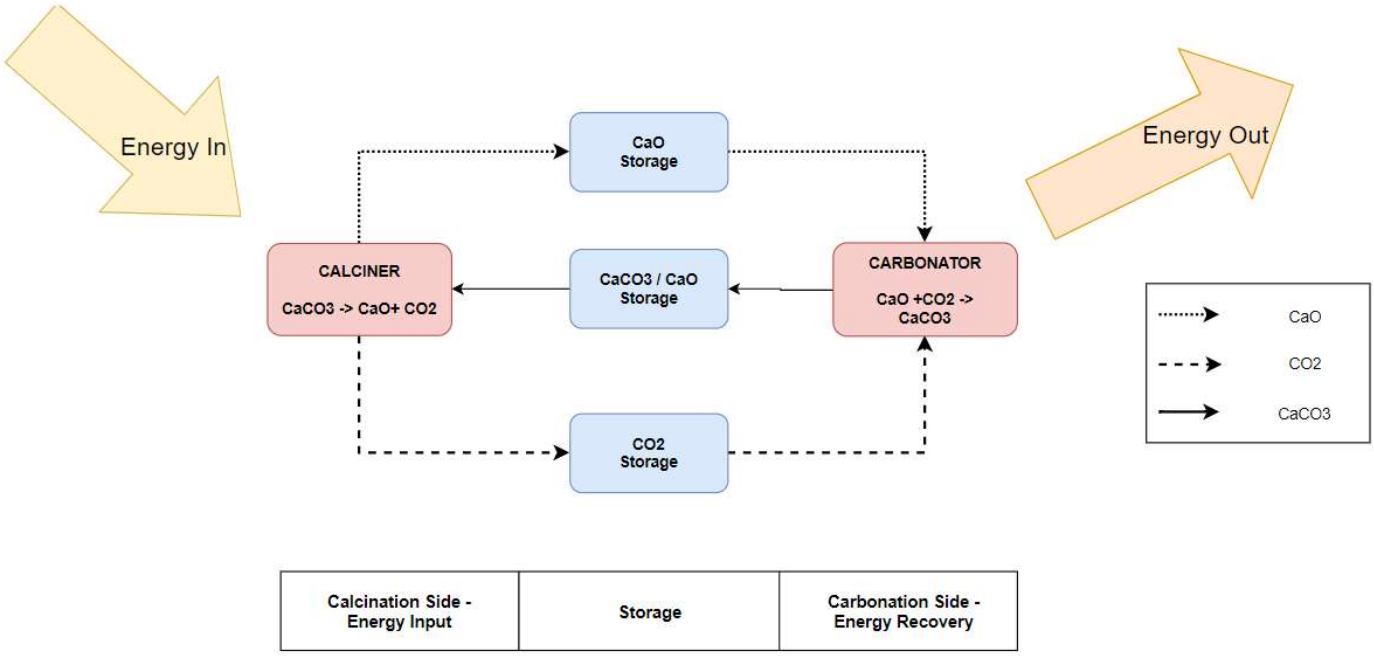

Figure 1 – Generalised Calcium Looping System Diagram using Limestone Precursor Material

Despite the recent increase of interest into CaL technology, studies of combined CC-TCES systems have not yet proved conclusive, with knowledge gaps surrounding the impact of various process parameters on the technoeconomic viability of processes in different applications.

1.2. Aim and Scope

1.2.1. Aim and Objectives

The aim of the project is to describe the energetic and economic balance of carbonate-cycles for simultaneous applications as carbon capture and energy storage and identify key aspects of process design from a technoeconomic perspective.

The following points divide the overarching aim into key specific objectives to meet the requirements of the final goal of the thesis.

1. To develop a detailed review of existing research into the CaL procedure at process level and identify existing knowledge gaps.

2. To design and construct a precise steady-state process model using Aspen+ software to analyse system performance under set conditions, outputting key process parameters including mass and energy flow rates and reactor sizing.

3. Detailed economic analysis through the application of Excel functions for economic modelling, outputting results through the use of the Net Present Value economic indicator for comparison.

4. Sensitivity analysis to determine the impact of process variables including material cycling rates and power output on the technoeconomic viability of the project.

1.2.2. Scope

This section outlines the scope of the project, including the system size and boundary conditions to be analysed.

The work focusses on the system at process level, as such the model that is developed considers the energy input and output as heat flows. The work does not consider the impact of reactor specific requirements and time variations on the charging and discharging sides. Maintaining the energy inputs and outputs, along with FG flows, as simple external values increase the number of situations for which the results are relevant. For example the power input source could be from the same power plant as the FG, or alternatively the system could be powered by a CSP plant, with the FG stream emitted from nearby industrial processes.

As the project is based on process modelling there are several associated assumptions involved which need to be accounted for when assessing the outcome of the work. The key components included within the model are operated in 'design-mode', with software approximating sizing as opposed to the values being input for a specific case. There are specific values assumed for various material properties based on literature research and solids-cycling effects.

The project focusses on calciner input power sizes in the scale of 100 MW-1 GW, this could be considered the range of heat available from a large CSP plant.

The project considers limestone as the sole carbonate precursor input. Limestone is the most widely studied CaL carbonate precursor due to its low cost and ready availability, as a result it is most likely to be used in future projects, keeping this work relevant. [24, 25]

This thesis has been carried out in collaboration with SaltX Technology, a company specialising in nanocoated salts for high temperature TCES. SaltX provided information for the definition of the material properties used in the model. SaltX Technology are supporting this research to better understand the technoeconomic impact of various parameters on the CaL system at process level.

2. Theory

2.1. Carbon Capture and Storage

2.1.1. Global CO_2 Emissions

Anthropogenic CO_2 emissions are widely regarded as the key contributor to climate change [26]. With atmospheric CO_2 levels expected to rise from 400 ppm in 2015 to 660-1550 ppm by 2030, assuming that no direct action be taken, temperatures will rise by 4.1-4.8°C [27]. 195 nations have reached an agreement to "combat climate change and unleash actions and investment towards a low carbon, resilient and sustainable future" at the 21st Conference of the Parties (COP21) held in Paris in 2015. This resulted in a goal to maintain global temperature rise to well below 2°C with an aim to reduce emissions in keeping with a 1.5°C temperature rise. This corresponds to limiting CO_2 concentrations within the atmosphere to 450 ppm by 2030. [28]

2.1.2. Mitigation Technology

A range of strategies exist to limit CO_2 emissions to the atmosphere, including shifting power generation from fossil fuels to renewable sources, efficiency improvements and, notably, CCS. Most mitigation scenarios incorporate a mixture of these technologies, with combined use of technologies such as CCS and biofuel power generation offering the potential of negative emissions. [29]

The decarbonisation of the energy and manufacturing sectors will prove difficult without the implementation of CCS technology, which has been proven to be one of the most viable methods of achieving a low carbon society. [30, 31] However, the cost of CCS technology is still one of the key limiting factors for its expansion to global energy markets. [31] Additionally, energy penalties in capture can limit system efficiencies and subsequently increase fuel requirement for the same power output. CCS systems typically require increased utility input, chemical flows and infrastructure costs associated with CO_2 transport, storage and utilisation. [32]

2.1.3. Carbon Capture Technology

Carbon Capture (CC) technologies are designed to selectively extract CO_2 from gas streams (generally FG in energy production or process streams from industrial processes), prior to either transportation for storage under super-critical conditions or repurposing to produce valuable products. [33]

CC technologies can be divided into three key process pathways (Figure 2) Post-Combustion CC; Pre-Combustion CC; and Oxyfuel Combustion. [12]

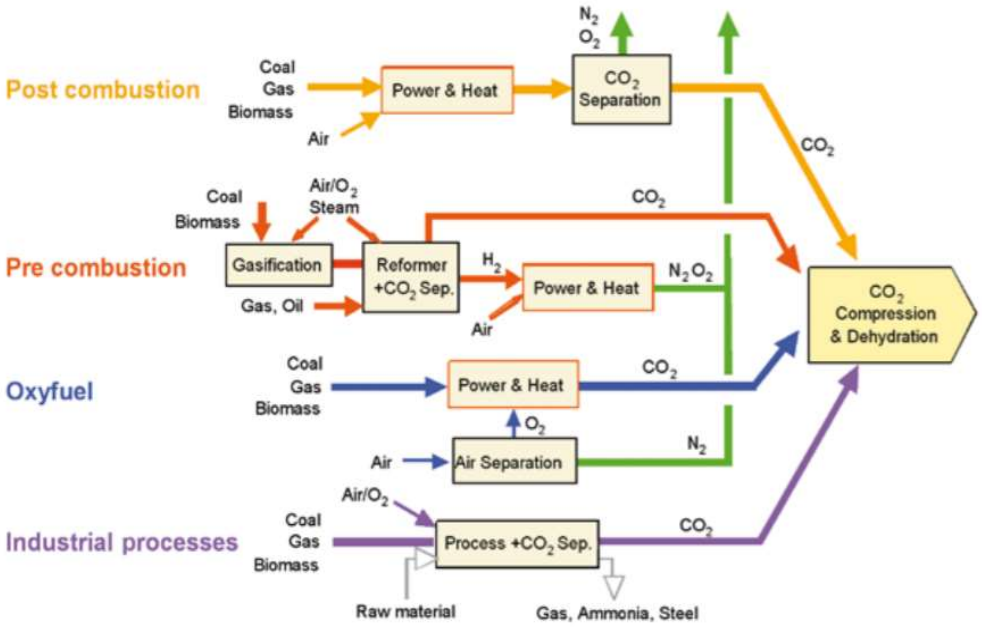

Figure 2: Carbon Capture Process Pathways [31]

Pre-Combustion carbon capture refers to the process of extracting carbon from carbon-based fuels prior to their combustion. Generally, pre-combustion processes involve the production of a purer carbon-based fuel from a traditional source, which can be combusted under a controlled environment to produce a CO_2-rich outlet FG. Other processes may focus on producing pure hydrogen streams for combustion from traditional hydrocarbon sources. [12]

Oxyfuel Combustion utilises pure oxygen in the combustion stage as opposed to air, resulting in an exhaust gas of an almost-pure CO_2-H_2O mixture, resulting in an easy-to-separate CO_2 stream. [12] Oxyfuel processes are capable of improving combustion conditions with rapid ignition from lower temperatures, reducing FG quantities at reactor exit and improved control of other emissions such as NOx. There are issues associated with the energy penalty in the production of a high purity CO_2 stream and managing the high combustion temperatures typical of combustion in a pure O_2 environment. [34]

Post-Combustion processes extract CO_2 from FG streams exiting combustion reactors, the most common of which involve chemical absorption or similar processes. [12] These processes are preferred for low CO_2 partial pressures, and are far easier to retro-fit to existing plants, they are generally driven by large heat demand. [35]

Post-combustion technologies are of particular interest in this project due to their retrofit-capability and relatively developed technology and are compared and further detailed below.

Absorption Based Carbon Capture processes dominate the CCS market [33]. Chemical-based processes generally make use of aqueous amine-based solvents or alkali solutions which react with CO_2 to form a weakly bonded compound, chemical absorption processes have high selectivity, and therefore are suitable for industrial FG applications. Physical absorption relies on Henry's Law and the partial pressure of CO_2 to combine with solvents (such as Selexol and Rectisol). [36]

Membrane Based Carbon Capture processes involve the separation of CO_2 from FG by pumping flow through a membrane, which selectively extracts gas based on diffusivity and solubility of CO_2 at separation conditions. The separation performance is influenced by the membranes material, configuration, morphology and composition. [37]

Adsorption Based Carbon Capture processes involve the addition of the CO_2 gas to a solid surface, the adsorbent is regenerated by heat generation or pressure decrease. Adsorbent materials commonly used for CC include activated carbon and metallic oxides. [36]

Chemical-Looping Combustion (CLC) and Reforming (CLR) Carbon Capture processes utilise metal oxides (MOx's) as oxygen carriers between separate air and fuel reactors. CLC processes fully oxidise feedstock in the fuel reactor, using oxygen transferred from an air reactor by the MOx particles (which are de-oxidised in the fuel reactor and re-oxidised in the air reactor in a continual loop). [38] CLR processes partially oxidise in the fuel reactor, and are primarily applied as means of hydrogen production. These processes produce an easily separable mixture of CO_2 and H_2O. [39]

Cryogenic Separation Carbon Capture extracts CO_2 from FG by condensation, reducing FG temperature to CO_2's condensation point (approximately -56.6°C at atmospheric pressure). This process is only feasible when CO_2 concentrations are high due to the cost of refrigeration, however, research has been undertaken to better thermally integrate systems with TES technology. [36, 40]

Table 1 [16, 24] summarises the comparison between *Calcium-Looping Carbon Capture* (introduced in Section 1.1), and the other CC processes described in this section. As seen in Table 1, CaL technologies can be identified as one of the most promising technologies for CC applications, primarily due to their retrofit capability, ability to recover heat, relatively simple operation, low environmental and economic impacts etc.

Table 1: Comparison of Post Combustion Carbon Capture Technology

Technology		Strengths	Challenges
Absorption Based CC [41, 36]	Physical Absorption	- Relatively high selectivity - Amongst most developed technologies	- Equipment corrosion - High energy penalties in the solvent-regeneration stage. - Environmental impact of chemicals used
	Chemical Absorption	- Relatively high selectivity - Amongst most developed technologies	- Amine degradation - Equipment corrosion - High energy penalties in the solvent-regeneration stage. - Environmental impact of chemicals used
Membrane Based CC [37, 42]		- Compact systems - Suitable for high CO_2 concentration streams	- Energy intensive - High cost of membranes - Low selectivity - Only feasible at low temperature - Prioritisation of either purity or recovery - Complex cycles - Specific extraction requirements - Multi-stage operation and require complex steam cycling.
Adsorption Based CC [36, 43]		- Promising research into improving adsorbent material selectivity	- Instabilities arising from impurities and moisture within FG - Low selectivity of adsorbent materials results in decreased feasibility for large-scale applications - High chemical material flow rate requirements
CLC and CLR CC [44, 45]		- Resistance to agglomeration - Low environmental impact of feedstock	- Complex material requirements from MOx - High Pressure requirements - Non-retrofittable - Only demonstrated at pilot scale
Cryogenics Separation CC		- Effective for high CO_2 content in gas (e.g., post oxyfuel combustion) - High capture rate	- High energy penalty in refrigeration if not integrated effectively -
CaL CC		- Potential for heat recovery TCES - Low cost of carbonate precursor - Low toxicity of precursor materials - Based on established principles from cement industry	- High material degradation - Poor selectivity of CO_2 over SOx

2.2. Energy Storage

2.2.1. Energy Storage Technology

There is a growing requirement for efficient energy storage to provide numerous grid services as energy systems decarbonise with increased integration of variable renewable energy technologies with varying temporal and diurnal loads. These include: grid flexibility; peak-load shifting and the provision of ancillary services such as frequency regulation [46, 47]

The electrical energy storage market is dominated by electrochemical and hydropower systems, which benefit from mature technology, high efficiencies and strong economic qualities, however concerns have been raised over their environmental impacts and long term sustainability. [48] As a result of these concerns and the growing demand for grid-level storage, focus on alternative storage technologies is once again increasing. [49]

2.2.2. Thermal Energy Storage Technology

There is a growing requirement for efficient, high-temperature thermal energy storage within energy systems for applications at thermal power plants, which can include load management in traditional fossil-fuelled powerplants and developing applications, for example peak-shifting in CSP plants. [50]

Efficient high-temperature TES systems have received increased attention in recent years which can be associated with the desire to reduce the demand on generation-side electrical energy storage (EES) systems. The disadvantages associated with conversion of thermal energy to EES include the environmental impact of traditional EES systems [11] and the high costs of electrochemical storage compared to traditional thermal storage technologies [49, 51].

The present project focuses on industrial process applications, as such high temperature storage technologies are of particular interest for comparison from the literature in order to provide process heat for steam generation and other applications. The primary high-temperature TES technologies implemented in industry can be classified as: Sensible Heat Storage (SHS); Latent Heat Storage (LHS) and Thermochemical Energy Storage. [50]

Sensible Heat Storage is the oldest and simplest form of thermal energy storage, typically having its foundations in low temperature energy storage solutions. Sensible energy storage has received increasing interest for industrial applications in the storage of high-grade heat [7]. The most common example of high temperature SHS utilised in industry is molten salt storage in CSP plants, these systems are popular due to low cost and environmental impacts. Molten salt storage operates by maintaining salts above their melting point in a storage tank and circulating them through a heat exchange system to a higher temperature storage tank from which they can later be discharged. The storage efficiency of these technologies is, like other thermal storage systems, primarily impacted by the conversion between thermal and electrical energy, with higher losses over longer storage times. Similarly the systems are typically high cost which may prohibit their widespread uptake. [52, 53]

Latent Heat Storage for industrial applications typically involves the use of Phase Change Materials (PCM), including, but not limited to: inorganic salts, metal alloys and organic materials, such as polymers. The basic concept involves heating a material to its melting or evaporation point, storing it at this temperature, and then solidifying or condensing the material to release the stored heat. This process takes advantage of the high energy content

resulting from the materials enthalpy of fusion or evaporation for high energy storage density across a relatively low temperature difference. [54]

Thermochemical Energy Storage technologies, introduced in Section 1.1, involve the reversible conversion of heat into chemical energy for storage, by facilitating the endothermic separation of a substance into two products that are stored separately to be recombined when heat is required. [8] These technologies have the advantages of: high energy storage density when compared to aforementioned alternatives; ambient temperature storage allowing storage over extended periods; transportability of stored energy; high discharge temperatures and subsequently higher efficiency in discharge cycles; and relative low cost of storage media such as limestone in comparison to systems such as metal alloy LHS. However, they face challenges associated with: degradation of storage medium and subsequently high material flow requirements; and typically are complex systems in comparison to alternatives such as SHS. [55]

Combined Phase Change Material (PCM)-CaL Systems, detailed by Wu et al., 2021 [56], combines system utilising a $CaCO_3$/CaO-$CaCL_2$ material in a PCM-CaL system, with the system storing heat as sensible, latent and thermochemical energy in the charging process through the melting of $CaCL_2$ and simultaneous conversion of $CaCO_3$. The $CaCO_3$ dissolves within the molten $CaCl_2$. The concept behind the combined system is both to increase the energy density of the storage system, enhance the energy transfer between the material in charge and discharge and to reduce the impacts of material degradation in the carbonation reaction.

2.2.3. Thermochemical Energy Storage Technology

TCES systems absorb heat by facilitating an endothermic reaction and separation of materials for storage prior to the release of energy in the process reversal as an exothermic reaction. A range of materials have been studied for use as energy storage media within TCES systems, these can be categorised into hydrides, hydroxides, carbonates, ammonia and metal oxides.

Metal-Hydride TCES systems utilise a reversible reaction between metal compounds, such as Mg-Ni or Mg-Fe, and hydrogen (forming Mg_2NiH_4 and Mg_2FeH_6 respectively). [57] They are capable of storing energy at approximately 2 MJ/kg. [58]

Oxide and Hydroxide TCES systems have drawn increased focus as candidates for TCES, particularly within the CSP industry. The key advantage of these systems is the production of a solid metal oxide and gas from the separation, both of which are easy to store. A typical metal oxide reaction is shown in Eq.2, where 'M' designates the metal, 'O' the oxygen content and 'h' the reaction enthalpy.

$$M_xO_{y+z} + \Delta h_{react} \leftrightarrow M_xO_y + \frac{z}{2}O_2 \qquad (Eq.2)$$

Various Metal Oxide systems have been demonstrated within the literature [59, 60, 4], utilising a range of MOx precursors such as Mn_2O_3 and Co_3O_4. These technologies have various benefits characteristic of TCES systems, however, they have no potential for CCS applications due to the lack of carbon atoms in the precursor materials used in typical cycles. [4]

Hydroxide based TCES systems store energy via the reversible endothermic separation of a metal hydroxide into steam and metal oxides. [61] Typical systems utilise compounds such as calcium hydroxide ($Ca(OH)_2$) and magnesium hydroxide ($Mg(OH)_2$), which are converted to steam with calcium oxide (CaO) and magnesium oxide (MgO) respectively. Calcium hydroxide

systems boast energy storage densities of 300 kWh/m^3 for operational temperatures between 4-600°C [62].

Investigation into hydroxide-based TCES has a greater relevance within this project, with the fluidisation of CaL systems by steam leading to the formation of $Ca(OH)_2$ as an intermediate effect of the calcination reaction, as is discussed in Section 2.3.1. [63].

Carbonate TCES systems utilise the energy released in the reversible reaction of carbonate materials. [55] Carbonates are the salts of carbonic acid (H_2CO_3), formed by the bonding of the anion CO_3^{-2} to metals, the most common of which is Calcium Carbonate ($CaCO_3$). [64] Carbonate processes cover a range of reversible reactions with the most common process being calcium looping systems (generally utilising limestone or dolomite precursors). The reversible carbonation reaction is detailed in Eq. 1.

Carbonate TCES systems are not limited to the use of calcium-based precursors, but have also been demonstrated with materials including $FeCO_3$ [55] and $ZnCO_3$ [65]. A comparison of different materials used in carbonation processes is detailed in Table 2:

Table 2: Comparison of carbonate precursor materials [55, 65, 69]

Precursor Material	**Chemical Formula**	**Energy Storage Density (GJ/m^3)**	**Enthalpy of extraction ΔH (kJ mol^{-1} CO_2 removed)**	**Operation Temperature (°C)**	**Cost ($/tonne)**
Limestone [66]	$CaCO_3$	4.489	165.8	> 880	10-60
Dolomite [67]	$CaMg(CO_3)_2$	1.944	125.8	~ 590	60
Magnesium Carbonate [67]	$MgCO_3$	3.396	96.7	~ 450	500
Iron Carbonate [68]	$FeCO_3$	2.6		180	
Strontium Carbonate [69]	$SrCO_3$	4	234	~ 1200	

The carbonates detailed can present issues associated with material degradation and sintering after multiple carbonation-calcination cycles. [66] As seen in Table 2, the reaction temperatures of several of the carbonate materials are unsuitable for high temperature heat recovery and high-quality steam generation, with low operational temperatures of materials including Iron and Magnesium Carbonates and unsuitably high temperatures of materials including Strontium Carbonate.

The low cost, operating temperature and high energy density of calcium carbonate make it ideal for applications as a thermochemical energy storage technology.

As mentioned in Section 1.1., this project focuses on systems that combine carbon capture and energy storage applications to optimise material and spatial usage. As such, carbonate-based chemical looping systems prove to be the only viable systems, separating CO_2 for storage from a carbonate in a reversible endothermic reaction, which provides substantial energy storage potential.

2.3. Calcium Looping State-of-the-Art

2.3.1. Calcium Process Description

CaL processes designs for combined TCES- CCS applications generally consist of two interconnected Fluidised Bed (FB) reactors, with intermediary storage, as displayed in the simplified process diagram (Figure 1).

The first of these reactors is designated as the carbonator reactor, where the CaO reacts with CO_2 in the FG to form $CaCO_3$, releasing heat. As the system intends to capture CO_2 from FG streams, the carbonator is expected to function based on the FG flow. This requires the discharge reactor to be able to operate steadily.

The second reactor is the calciner reactor, within which the solids are regenerated to form CaO and CO_2 with the addition of heat. In combined CC-TCES systems, the calciner typically only operates when an excess of energy is available, hence the system 'charges'. [7] In cases where external VRE sources, such as a CSP plant, are utilised this may be an 8-hour period.

2.3.1.1. Carbonator

The exothermic carbonation reaction takes place between 600-750°C, with reactions taking place at approximately 650°C at atmospheric pressure. [70, 71] The exothermic nature of the reaction results in the requirement for continual heat extraction to maintain reaction temperatures.

Residence times within the carbonator must be focussed upon maximising CO2 capture rates, the literature has shown that reaction periods within the range of 5-10 minutes can achieve capture rates of up to 90%. [72]

The efficiency of CaL processes for CC are reduced by the unavoidable constraint of low CO2 partial pressure within the FG. [56] It is possible to adjust internal reactor pressures, however, there are logistical issues and energy penalties in the compression of FG streams. [73]

2.3.1.2. Calciner

The regeneration of CaO from $CaCO_3$ takes place in the calciner reaction, absorbing heat in an endothermic reaction. Calcination reaction temperatures typically depend upon the physical and chemical make-up of the carbonate, and the partial CO_2 pressure within the reactor. [74]

Operational temperatures within the calcination reaction have been widely studied in order to reduce the impacts of sintering and subsequent particle deactivation, and studies have shown that temperatures between 900-950°C are the optimal for heat release whilst maintaining particle activity. [75]

The efficiency of the process as a whole is drastically affected by the concentration of CO2 within the calciner reactor. High partial-pressures of CO2 leads to notable deactivation of CaO after only a few cycles. However, there are notable benefits to operation at higher pressures, requiring smaller reactor sizes, more efficient removal of fluidisation agents such as steam, and can potentially lead to improved reactions through smoother operation with less internal bubbling and higher dense phase voidage – leading to improved heat and mass transfer. [76] Due to the inconclusive evidence surrounding calcination pressure, studies of the process that do not consider reaction kinetics and effects typically use atmospheric pressure values. [71]

The process utilises FB reactors, as such there is a requirement for a fluidisation agent, detailed in Section Fluidisation Agent The process gases within the calcination stage are released from the solid particles and as such provides limited initial fluidisation effects.

2.3.1.3. Precursor Materials

Limestone and dolomite are the most widely studied precursor materials used in the CaL process. [45, 67, 70, 77] Although there has been some investigation of alternative natural carbonate sources, such as those derived from animal bi-products including bird eggshells and shellfish [66], there is a general lack of data regarding their behaviour following repeated cycling. [78]

2.3.1.4. Particle Deactivation

A loss of material CO_2 sorption capacity has been observed in numerous studies as the number of calcination-carbonation cycles increases. [14, 45, 79] Evidence has shown that activity of limestone can half within 10 cycles of calcination/carbonation in an inert atmosphere (Figure 3), dropping to 7-8% after thousands of cycles [80]. This is primarily associated with the sintering of the material and hence loss of porosity within the particles, greatly impacting on particle activity [76].

The temperature and residence time within the calciner reactor have been found to have the largest impact upon particle sintering – long residency at high temperature notably increases material sintering effects. [75] Similarly, material particle size and origin can have an effect on the deactivation behaviour during cycling, the impact of these variables can be associated with the capability of the CO_2 to reach and react with surface CaO, this is more significant than the influence of CO_2 partial pressure during carbonation [75].

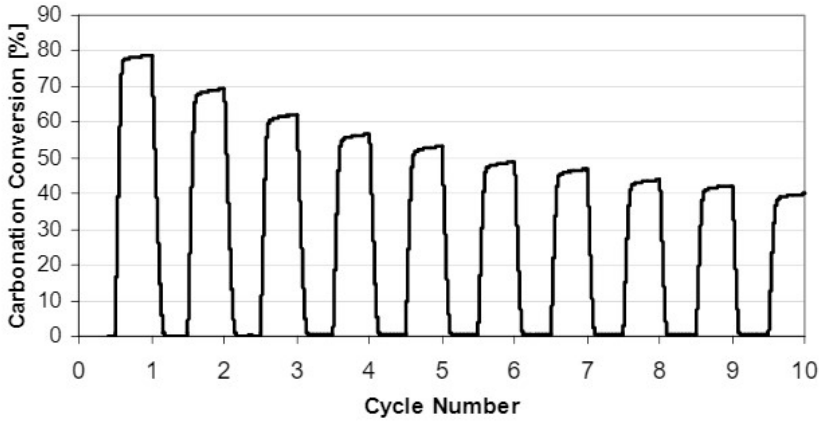

Figure 3 – Loss of sorbent activity during CaL cycles with 60-minute calcination and carbonation (700°C) residency in inert N_2 atmosphere. [80]

Additionally the CaO sorbent material can react with SO_2 within FG to produce $CaSO_4$, which hinders its potential for CO_2 sorption. [24] Further, mechanical effects, such as attrition following repeated cycling, can result in material losses and changes to sorbent surface structures – both of which may impact particle activity. [78]

Maintaining high material activity is essential within CaL systems as, despite the low cost of precursor materials, sorbent replacement is one of the largest economic influences upon the viability of systems. [81] Methods for improving particle activity have been studied at length,

with some of the most promising methods including nano-coating of particles and steam-regeneration of oxides. [63, 80]

The deactivation and attrition of material sorbents makes it essential to run the systems with purge and make-up flows in order to maintain efficient reaction conditions, even if improved reactivation processes are used – as these are typically not 100% effective. [80] Purge flows aim to maintain an average particle activity to ensure reasonable CO_2 capture efficiency, this is achieved by setting a target average cycle number (or activity) and back calculating the inflow/outflow of solids to achieve this. These calculations are reviewed in greater detail in Section 3.2.3.

2.3.1.5. Fluidisation Agent

CFBs are typically operated with gas velocities in the range of 5-10 m/s [82], with a range of alternative agents available. The addition of an external fluidisation agent is required solely within the calcination process, as the only fluids present within the reactor are reaction products which are incapable of providing the initial fluidisation requirement. The flue gas present in the carbonation stage should prove sufficient to produce fluidity effects upon particles.

Typically, calcination reactions have been fluidised by use of either an fully inert fluidisation agent [83], or through the use of steam, which has some impact upon the reaction behaviour within the system. [84] Jayarathna et al., 2015, proposed a system where a steam fluidisation agent is utilised in a 1:1 ratio with the predicted CO_2 emittance. The steam and CO_2 exiting the process are separated by means of H_2O condensation. [84]

Process modelling of steam-fluidised calciners has generally failed to consider the impact of steam presence on material activity during cycling [84, 85]. The impact of steam presence on calcination has primarily been studied in cases where steam forms part of the fluidisation mixture, alongside inert gases such as nitrogen. [63] It has been seen that the injection of steam at relatively low partial pressures can have a marked improvement upon material activity following numerous cycles [86]–[88].

Champagne et. al. [87] have demonstrated the impact of steam during calcination under a range of fluidisation conditions. Figure 4 demonstrates the impact of varying steam concentration within the fluidisation mixture, with N_2 and CO_2 forming the rest of the fluidisation mixture within the reactor. It can be seen that a mixture of 15% steam, 25% Nitrogen and 60% CO_2 has the largest beneficial impact on the residual conversion percentage after 15 cycles. However, fluidisation using steam as the sole fluidisation agent (40% steam, 60% CO_2 within the reactor) has been demonstrated to have an improvement of approximately 5% on the overall conversion extent (%). [87]

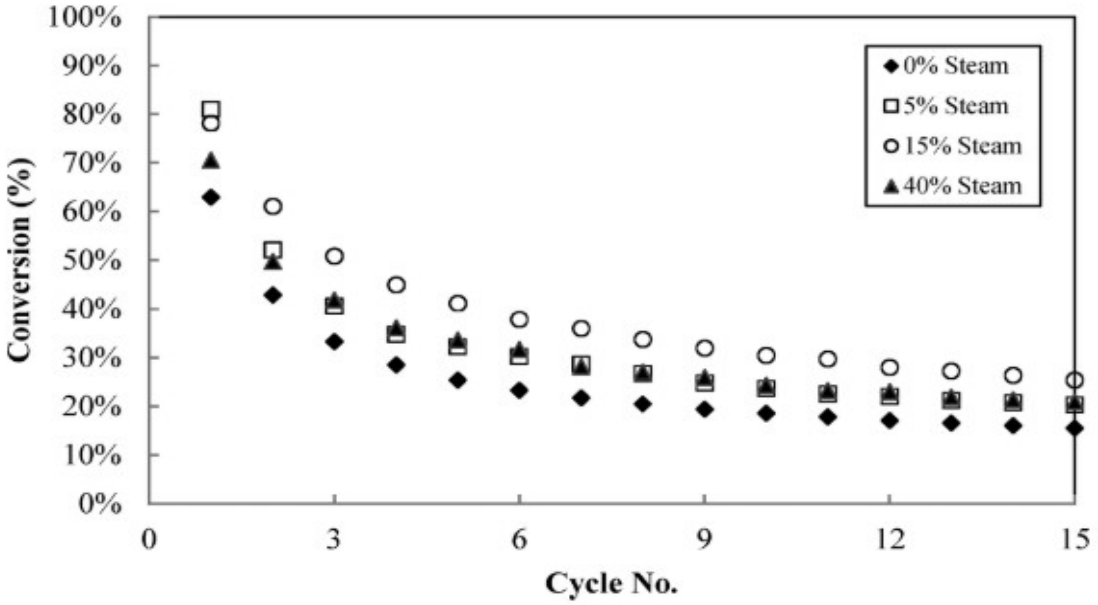

Figure 4 - Carbonation conversion from TGA tests performed on Cadomin limestone (250–425 μm) with calcination at 925 °C, 60% CO2, and varying steam concentration (balance N2) followed by carbonation at 620 °C (15% CO2, balance N2). [85]

Calcination conversion temperatures are substantially higher than those used in steam hydration of CaO, however, evidence has suggested that transient surface hydration effects within the calcination stage result in a change in the sorbent morphology, which can increase the particle activity. [89]

Varying the molar concentration of fluidisation gas within the reactor to 40% reduces the CO_2 partial pressure to 0.6 atm (for a reaction taking place under atmospheric pressure conditions). This results in a variation in the equilibrium calcination temperature. The equilibrium calcination temperature describes the minimum temperature at which it is possible for calcination to take place at a set CO_2 pressure, and has been studied in depth. [90, 91]. Ebneyamini et. al. [92] provide a simplified graph (Figure 5) from which the minimum

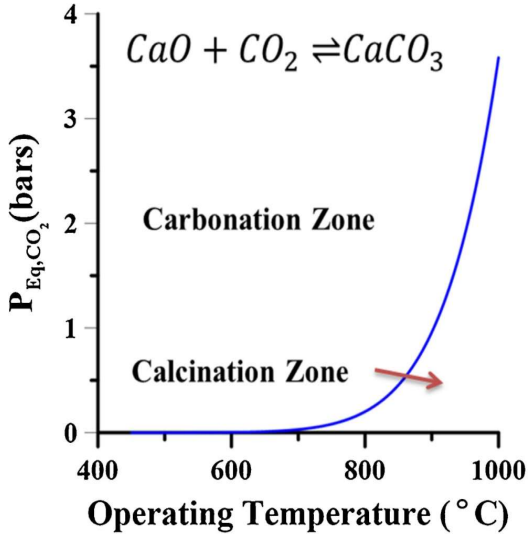

Figure 5 - Calcination-Carbonation Equilibrium Curve

equilibrium temperature of calcination can be determined as above approximately 875°C. This is well below the calcination conditions quoted by Champagne et. al. [87] for steam fluidised calcination (925°C).

The presence of steam within the carbonation stage has been noted as having an effect on the particle activity following repeated cycling, however evidence of its impact has proved inconclusive within the literature. [89, 93, 94]

2.3.1.6. Storage Conditions

Both the intermediary solids storage and final CO_2 storage conditions have a major impact upon the overall efficiency of the system.

CaL systems with combined TCES-CCS purposes, defined in the literature, do not recirculate CO_2 flows, as such CO_2 flows exiting the system are cooled and compressed to industry standard storage conditions. [6, 12]

Solids-storage conditions are highly dependent on the requirements of the system, with ambient ("cold") storage conditions common within the literature for TCES-systems [84, 95]. Cold storage systems have the advantage of long storage times with low heat losses and the potential for easy transportability of stored chemical energy, however, hot-storage systems have the potential to reduce heat exchanger requirement and hence investment costs. Additionally, the lack of requirement for high temperature differences between reactors and storage vessels can reduce losses within systems requiring heat exchange over large temperature differences.

2.3.1.7. Heat Exchangers

To optimise CaL processes for TCES-CCS applications, it is essential to increase their thermal integration. This is particularly important in systems utilising cold storage technology, where the high temperature difference between storage and charge/discharge can result in greater losses if improperly integrated [13].

HX networks within CaL processes can be complex, requiring the integration of a mixture of gas-gas, gas-solid and solid-solid HX, and potentially liquid-solid or liquid-gas HX's depending on the fluidisation agent utilised in the calciner. [84]

HX design, for example, gas-solid and liquid-solid HXs, are relatively well developed within industry, [96]. However, solid-solid HX design remains poorly covered within the literature, and generally involves the use of an intermediary fluid to act as a heat exchange medium between particles, although designs involving conduction through a plate do exist [97].

2.3.2. Techno-economic Assessments of Calcium Looping Systems

Combined TCES-CCS applications of CaL systems is a relatively new field of study, with process modelling and economic analyses in the literature primarily focussing on individual TCES or CC systems [7, 24, 95].

The studied literature includes several studies of properties of materials relevant to CaL systems, investigating the impact of different precursor materials [67] and regeneration methods [63, 66, 89, 98]. However, the studies reviewed within the literature have not

considered the economic impacts of regeneration at a process level for technoeconomic analysis.

Studies have detailed the impact of varying make-up flows on average particle activity, providing insight into the calculation of required system flow rates. [14] These calculations have been considered within process models of CC only systems, however their impact has been reviewed in limited depth for TCES and combined TCES-CCS systems.[14, 22] Notably, there is a lack of consideration of varying particle cycle rates for fixed deactivation constants on the economic and energetic balance of combined systems within the literature.

A range of process modelling software have been demonstrated for the description of calcination/carbonation cycles, considering reaction kinetics and fluidisation effects on a range of Computational Fluid Dynamic software and programmes such as MatLab [23, 99]. The most common method used is either Aspen+ software or Aspen HYSYS due to their in-built databases describing reaction conditions. [83, 84]

3. Methodology

This section details the methodology followed in the completion of the project. The process flow diagram depicted in Figure 6 - Methodology flow-diagram demonstrates the interaction between data sources, highlighted in purple and the key stages of the process design and modelling. Initially, the core process is defined based on the findings within the literature, following which material and reaction properties are extracted and input into the model. Following the initial process modelling an economic analysis is undertaken, followed by a sensitivity analysis for two separate cases. The final stage of the project is based on the collation and analysis of the models results.

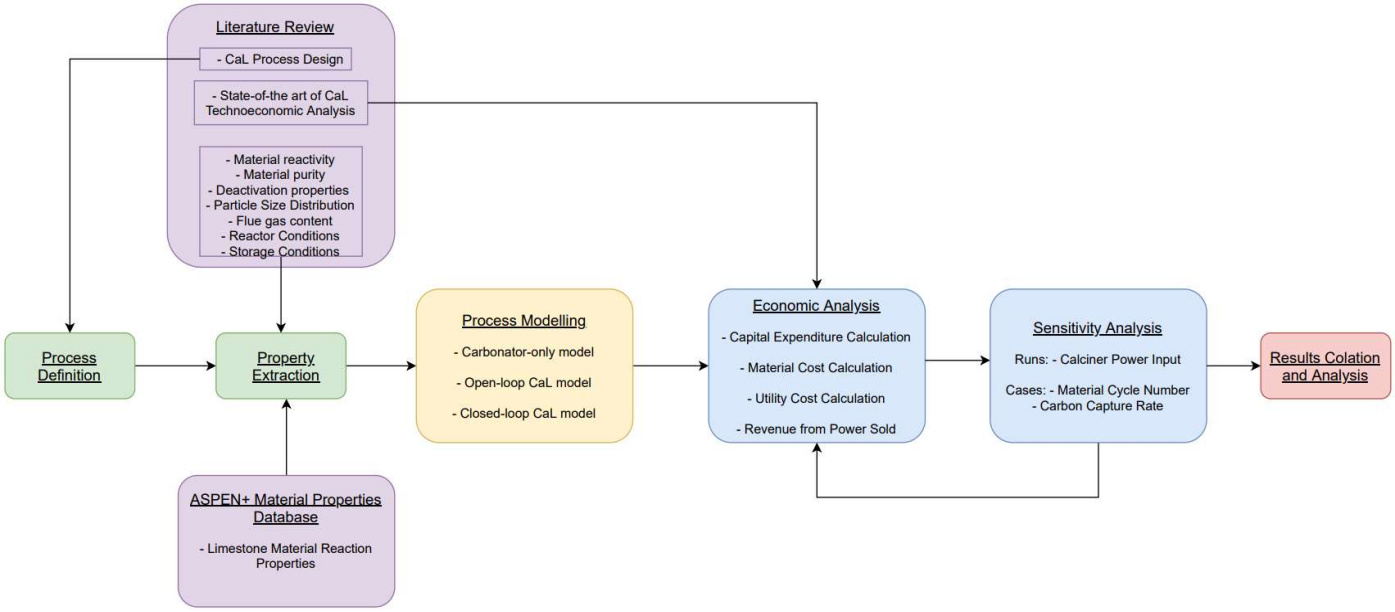

Figure 6 - Methodology flow-diagram indicating: process design stages (green); data sources (purple); process modelling (yellow); further analysis (blue); and results collation (red)

The literature review is conducted to outline the current state-of-the-art in the design of CaL TCES-CCS processes, which is used to develop a process model. The literature provides recommended values for some of the system inputs, in combination with Aspen+'s inbuilt material databases for the reaction products and energy release.

The process modelling undertaken in this work seeks to define the internal mass and heat flows within the system, including losses, material purge and make up flows, subsequently calculating the economic impact of various cases. The model is developed using Aspen+ software to define a steady-state model of the process. The modelling is undertaken in three stages, with first the construction and running of a carbonator-only model, followed by an open loop model without storage or recirculation followed by a final detailed closed loop model. The model is linked to an Excel spreadsheet calculating the required mass flows to maintain activity for specific cycles, simultaneously Aspen outputs values for the dependent variables to the spreadsheet.

The development of a CaL model on Aspen+ involves the following stages:

- Property method selection

- System component specification (material definition, with the identification of conventional and non-conventional components)

- Process flowsheet design (implement unit operation blocks and connect material and energy streams)

- Specify stream flow rates, composition and thermodynamic conditions

- Specify unit operations (set chemical reactions and thermodynamic conditions according to block requirements)

- Process optimisation (implement manipulator blocks, such as design specs and calculator blocks, in order to optimise process for variable inputs)

Aspen+ was used to determine accurate values for energy produced/consumed within the carbonation/calcination cycles for the pre-set material activity values. These outputs were extracted and implemented within the excel file for accurate cost calculations and reactor sizing.

Heating and cooling requirements were determined by the Aspen+ model, an accurate pinch analysis was undertaken utilising the Pro-PI Excel add-in. The Pro-PI software is then used to construct a stream-representation diagram to determine the most efficient heat integration of the system. HX loads and utility requirements can then be estimated by following the basic rules of pinch analysis. The HX's were not modelled and sized due to time constraints and lack of standardised design for solid-solid heat exchangers, which would likely have led to inaccurate results.

The economic analysis was undertaken using Excel software, allowing the calculation of operational costs and revenues, and the capital expenditure in reactor construction. Excel is preferred to Aspen+'s inbuilt economic simulator for reactor design due to its potential for greater control over cost equations.

Following the design and run of the base models a sensitivity analysis was undertaken in order to assess the impact of particle cycling and carbon capture rate (X_{CO2}) on the financial and energetic balances of the system.

The model allows the identification of the optimal economic balance between costs associated with sorbent injection-rate/make-up flow and the energy penalty associated with reactivating degraded sorbent material to provide a net present value (NPV) for various cases.

3.1. Process Description

This section briefly details the key principles of the CaL process identified within the literature which are essential in the development of an accurate process model.

A basic representation of the investigated CaL process for combined CC-TCES displayed in Figure 7. This system forms the basis of the process modelling described within Section 3.2.

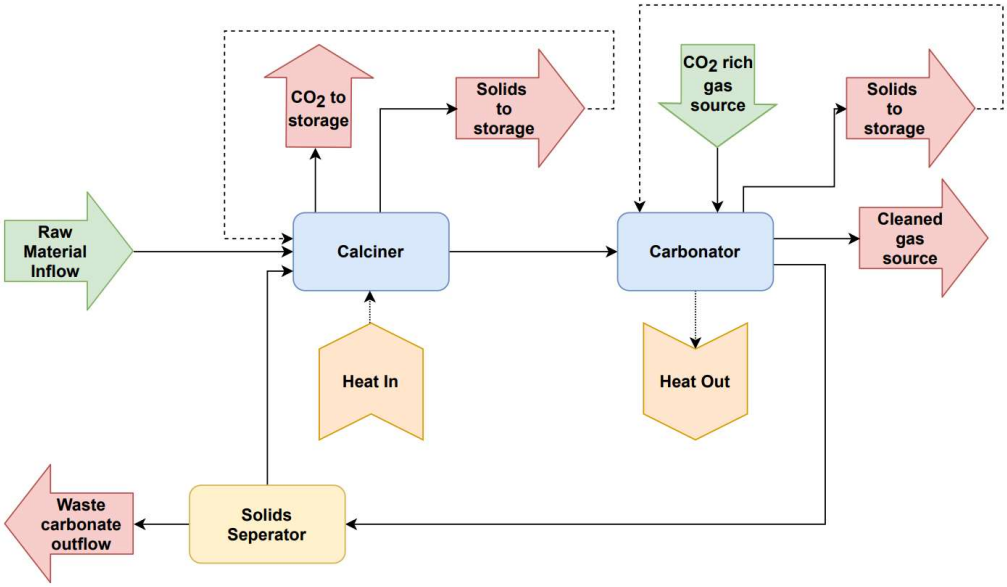

Figure 7 - Basic CaL process flow diagram signifying process inflows (green), outflows (red) reactors (blue) and heat flows (orange)

Figure 7 displays a closed-loop CaL process, with solids circulating between the calciner and carbonator, with a carbonate inflow and waste outflow demonstrated. A fluidisation agent inflow is required into the calciner reactor, not pictured. Due to the varying conversion rates within the calciner and carbonator the composition of solids flow within the system will not be uniform, i.e., the solids flow will be a mixture of CaO and $CaCO_3$.

The potential for solids-storage is depicted at the calciner exit, alongside the CO_2 exit flow. Although the potential for recirculation of stored solid is indicated within the process flow diagram, this is not modelled within the present work.

A basic heat inflow is indicated as a calciner input, with heat outflow from the carbonator.

In this process a steady flow of CO_2 rich gas into the carbonator is indicated, with a 'cleaned' (targeted CO_2 concentration removed) gas flow exiting the reactor.

3.1.1. Key process assumptions

The key assumptions included in the process definition relate primarily to the reaction conditions and properties/composition of inflows. The material reaction behaviour is determined by Aspen+'s in-built properties database.

The reactions are both considered to take place at atmospheric pressure, with temperatures with in the calciner set at 925°C and carbonator at 650°C, according to the literature. [85, 87]

The reaction stoichiometry within the reactors is set according to values extracted within the literature for reaction extent. The fractional conversion of $CaCO_3$ to CO_2 and CaO is set at 0.95 within the calciner [90]. The conversion of CaO to $CaCO_3$ with the addition of CO_2 is initially set at 0.7 within the carbonator [22], this value is adjusted to consider the effects of particle cycling discussed in Section 3.2.3.2.

FG composition and temperatures are extracted from the literature, based on industry standard values for coal combustion. An FG inflow temperature of 300 °C is assumed, with a mass-flow composition of 10% CO_2, 3% O_2, 69% N_2 and 18% H_2O [100]. An exit flow temperature of 300 °C is also assumed, this is higher than standard exit temperatures following treatment, and is taken as the heat recovery side of the system is not considered.

The final key assumption within the model development is the storage conditions of both solids and gases. It is assumed the solids are be stored at ambient conditions (atmospheric pressure and 20 °C). The CO_2 stream exits the process at industry standard conditions of 16 atm and -17 °C [101].

3.2. Model Development

This section details the development of an accurate model of the CaL system using a combination of process simulation and economic analysis.

3.2.1. Process Simulator: Aspen Plus V11

Aspen+ is a proven and acceptable process modelling software for solids-cycling applications [84, 99, 102]. It encompasses a large property database of conventional materials and compounds, allows user customisation of reactor blocks and contains detailed convergence algorithms for process optimisation.

Aspen+ lacks a specific fluidised-bed reactor model, however this can be simulated by modifying a r-CSTR block. For the purposes of this study kinetic effects are considered within basic assumptions related to particle cycle times and reaction rates [103] built into external calculations, however specific reaction calculations are not included within the model.

3.2.1.1. Physical Property Method Selection

The choice of property method is largely dependent upon the components present within the system, in this case a mixture of gases, liquids and non-conventional solid components. For this reason, a solids property method is selected, as this considers specific governing equations for fluids (calculated using an 'IDEAL' property method) and non-conventional solids [104].

The solids property method segregates fluids into a 'MIXED' sub stream and solids into a 'CIPSD' sub stream, and treat them with the corresponding governing equations. The property models used in CIPSD sub streams consider pure component properties of the polynomial type.

3.2.2. Process Modelling Calcium Looping

This section details the reasoning behind the use of each block in the model, the process flow and the inputs to each block.

3.2.2.1. Component Specification

The CaL system design requires the use of a mixture of conventional and non-conventional components. The CO_2, N_2, H_2O and O_2 materials are modelled using Aspen+'s 'conventional' material database. The CaO and $CaCO_3$ components are modelled using the non-conventional solids database.

3.2.2.2. Block Selection

Both the calciner and carbonator reactors are modelled as RStoic reactor blocks. These blocks allow the implementation of stoichiometric reaction values in cases where reaction kinetics are unimportant or unknown, as is the case in this model.

Simple splitter blocks are used to split the purge flow from the material recirculation and to separate CaO for storage. Similarly, a simple mixer block is used to combine the make-up and recirculating $CaCO_3$ flows.

Cyclone blocks are used to separate CO_2-H_2O gas from the CaO solids flow at the exit of the calciner, and to separate clean flue-gas from $CaCO_3$ at the exit of the carbonator. Cyclone blocks are preferred to simple solid separators as they provide greater control over separation efficiencies and sizing at the given Particle Size Distribution (PSD).

A Flash2 separator is used to separate condensed H_2O from CO_2 calciner exit. Flash2 blocks are able to perform rigorous two (vapour-liquid) or three (vapour-liquid-liquid) phase equilibrium calculations, producing a vapour stream and a liquid stream at outlet.

Heating and cooling loads are simulated using the simple 'Heater' block, which models one side of a HX, providing the capability for single and multiphase calculations.

Design-Spec blocks are implemented to vary the steam flow entering the calciner reactor to ensure the correct volumetric flow rate is achieved for fluidisation, and to vary the FG flow to achieve the required carbon capture rate given the material flow within the circulating system.

Calculator blocks are implemented within the model to apply external calculations extracted from Excel spreadsheets into the flowsheet computations.

3.2.2.3. Model Construction

A simplified model scheme is shown in Figure 8, for simplicity this schematic does not include Heater blocks. A more detailed diagram of the model is presented in Appendix A. The specific model inputs are detailed in 'Appendix B'. These inputs were extracted from the literature, as described in Section 3.1.1, the justification of specific variables is detailed in this section.

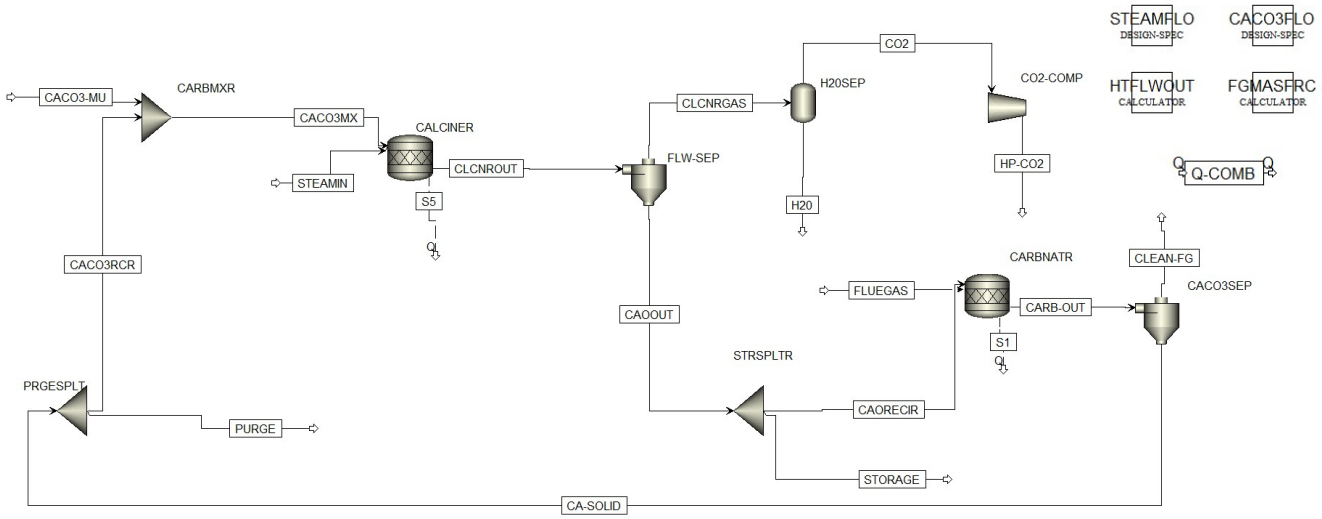

Figure 8- Simplified Aspen model sequence displaying key blocks in process design, not including heat flows

The calcination reaction takes place within the 'CALCINER' block and the produced CaO, CO_2 flow to a separator block, with the fluidisation agent ('CLCNROUT' stream). Table 5 in Appendix B provides details of the inputs into the reactor block, with the key process assumptions for the calcination reaction, detailed in 3.2.2.1 input here.

The 'FLW-SEP' cyclone block separates the solid CaO material from the CO_2 and H_2O vapour. The steam is separated from the extracted CO_2 by means of a FLASH2 separator block, 'H2OSEP', the CO_2 then passes through a compression stage for storage. The inputs into Flash2 block 'H2OSEP' are based on steam condensation properties [84].

The solids exiting 'FLW-SEP' are separated for storage or recirculation by means of a simple splitter block 'STRSPLTR', with the recirculated CaO feeding into the 'CARBNATR' RStoic reactor, where it reacts with the CO_2 content in the 'FLUEGAS'. The exit flow from the carbonator 'CARB-OUT' is separated by means of another cyclone 'CACO3SEP', with cleaned FG being emitted to the environment and $CaCO_3$ recirculatied. Table 6 of Appendix C details the inputs into the respective splitter and mixer blocks. The inputs into both Cyclone blocks, 'FLW-SEP' and 'CACO3SEP', are based on general assumptions for cyclone separators to handle large mass flows. The cyclones operate in design mode to allow accurate sizing based upon required separation efficiencies for cost calculation.

Table 7 in Appendix C details the inputs into the compressor block 'CO2-COMP'.

The recirculating solids stream is separated into a 'PURGE' flow and a recirculation stream 'CACO3RCR' flow by means of a simple splitter block 'PRGESPLT'. With the remaining carbonate being mixed with a make-up flow in the simple mixer block 'CARBMXR'. This flow then feeds back into the calciner, closing the loop. The inputs into the FMixer block 'CARBMIXR' (Table 6) allow the convergence of the mixing between the two streams with limited computational requirement.

Table 8 of Appendix C displays the HX requirements, these values are based on the temperature requirements of reactor blocks and storage conditions, detailed in Section 3.1.1.

The 'STEAMFLO' Design-Spec block is required to control the steam mass flow rate into the calciner to ensure that the targeted molar concentration of 40% steam and 60% CO_2 is maintained within the reactor to validate activity assumptions. [63]

The 'CACO3FLO' Design Spec block varies the FG flow rate into the system based on targeted CO_2 capture rates within the carbonator for a set solids recirculation flow. For a set reaction extent within the carbonator a limited quantity of CO_2 is combined with CaO inflow, to ensure that the FG entering the system experiences the pre-determined capture rate its flow rate must be adjusted.

The detailed inputs into the two Design-Spec blocks are provided in Table 9.

The 'FGMASFRAC' calculator block maintains the FG mass fractions at the required quantity [100], without this calculator block the 'CACO3FLO' block would solely modify the CO_2 flow within the FG, as opposed to the total mass flow.

The 'HTFLWOUT' calculator block contains a detailed excel spreadsheet where model outputs are collected for external analysis. Additionally, this calculator block sets the make-up mass flow into the system, which (in combination with the split-fraction in the 'PRGESPLT' block) is required for the specification of the mass flows within the system. These values are based on external calculations for the model inputs.

Table 10 of Appendix C provides a detailed description of the values input into the two calculator blocks.

3.2.3. External Calculations

This section details the concepts behind the external calculations implemented into the Excel worksheet, which set the internal mass flow rates.

3.2.3.1. Internal flow rates

The internal mole flow of the system ($\dot{m}ol_{CaC}$) is calculated based on the heat input to the calciner. The heat flow ($\dot{Q}$) input converts a corresponding quantity of $CaCO_3$ based on the calcination extent ($\eta_{calciner}$) and reaction enthalpy ($\Delta h_{calcination}$).

$$\dot{m}ol_{CaCO} = \Delta h_{calcination} \times \eta_{calciner} \times \dot{Q}_{input} \qquad (Eq.3)$$

The mass converted per unit time is a fraction of the total internal inlet flow. The raising of reactor inputs to reactor temperatures is externally from the reactors by a series of heat exchangers, as such raising inputs to reaction temperature does not have to be considered within this calculation.

3.2.3.2. Particle activity

A reduction in carbon capture and energy storage capability is expected following repeated carbonation-calcination reactions. [74, 105–107]

The fraction of CaO (reactive material) in a particle after each cycle can be defined as the carbonation conversion X_N. Equation 4 displays a general equation to calculate carbonation conversion, a function of the number of cycles N, deactivation constant k and the residual conversion of CaO expected following infinite cycling X_r [77, 105]:

$$X_N = \frac{1}{\left(\frac{1}{1 - X_r}\right) + kN} + X_r \qquad (Eq.4)$$

The system is modelled for continuous operation, with a flow of solids separated for storage. A number of particles undergo partial carbonation across multiple cycles, as such the particles performing a cycle at a given point experience a varied range of deactivation.

A make-up flow is required to maintain average particle activity within the process. Equation 5 estimates the fraction of particles carbonated N times 'r_N' within the cycle, this is dependent on circulation (F_r) and make-up (F_0) rates [108]:

$$r_N = \frac{F_0(F_R)^{N-1}}{(F_0+F_R)^N} \qquad (Eq.5)$$

From which the average particle activity within the system, X_{AVE} can be found [108]:

$$X_{AVE} = \sum_{N=1}^{N=\infty} r_N X_N \qquad (Eq.6)$$

Assuming incomplete reaction of particles within each CFB, the carbonation fraction f_{carb} and calcination fraction f_{calc} within each reactor for a specific cycle can be defined, based on material properties X_{carb} (carbonation extent) and X_{calc} (calcination extent), with the adjusted activity from X_{AVE}:

$$f_{carb} = \frac{X_{carb} - X_{calc}}{X_{AVE} - X_{calc}} \qquad (Eq.7)$$

$$f_{calc} = \frac{X_{carb} - X_{calc}}{X_{carb}} \qquad (Eq.8)$$

Rodriguez et al. [14] show that, for a specific number of cycles, N_{age}, the fraction of CaO present in the carbonator r_{Nage} can be calculated:

$$r_{Nage} = \frac{\left(r_o + \frac{F_0}{F_R}\right) {f_{carb}}^{Nage-1} {f_{calc}}^{Nage}}{\left(\left(\frac{F_0}{F_R}\right) + f_{carb}f_{calc}\right)^{Nage}} \qquad (Eq.9)$$

Where r_0 represents the fraction of $CaCO_3$ within the system that has remained uncalcined throughout the process for a given cycle.

The average activity can be calculated from material degradation properties using [14]:

$$X_{AVE} = (F_0 + F_R r_0) f_{calc} \left(\frac{a_1 f_1^2}{F_0 + F_R f_{carb} f_{calc}(1-f_1)} + \frac{a_2 f_2^2}{F_0 + F_R f_{carb} f_{calc}(1-f_2)} + \frac{b}{F_0}\right) \qquad (Eq.10)$$

Where the following symbols signify numerical indicators: a_1=0.1045; a_2= 0.7786; f_1=0.9822; f_2=0.7905; b=0.07709.

Detailed reactor design is beyond the scope of this project; therefore reactor sizing is not considered in the determination of targeted average particle activity. The average particle activity following multiple cycles is therefore approximated at X_{AVE}=0.6, based on information provided by SaltX – in line with values extracted from the literature [19], this

value is lower than the targeted activity used in the base case (one particle cycle), which is set by material specific properties.

The required purge and make-up flow rate to achieve this activity can be calculated by rearranging Equation 10 to give:

$$F_0 = \frac{r_0 F_R f_{calc} b a_1 f_1^2 a_2 f_2^2 - X_{AVE}(F_R f_{calc} f_{carb} b\big((1-f_1)a_2 f_2^2 + (1-f_2)a_1 f_1^2\big))}{X_{AVE}(a_2 f_2^2 b + a_1 f_1^2 b + a_1 a_2 f_1^2 f_2^2) - a_1 a_2 f_1^2 f_2^2 b} \qquad (Eq.\,11)$$

This value shall vary for targeted particle recirculation rates and the calculated mass flow rate into the calciner to achieve the given heat input for each simulation.

3.2.3.3. Reactor Conversion

The reaction extent of CaO within the carbonator varies depending upon cycle number, to ensure the model considers molar flows of deactivated material. The deactivated material is modelled as recirculating CaO within the system. The fractional conversion within the carbonator is therefore adjusted to consider the mass flow of deactivated material as a non-reacting CaO flow.

No adjustment is made within the calciner, as the reactor is still capable of converting 95% of $CaCO_3$ into CaO, rather the quantity of $CaCO_3$ entering the reactor reduces as a result of the change in the cycle number.

3.2.4. Heat Exchanger Modelling

A simple Pinch Analysis was undertaken using the Pro-PI Excel add-in. Pro-PI software allows the generation of stream representation diagrams and various composite curves to identify optimal heat integration. This analysis allows the calculation of heat recovery potential for each case and the determination of heating and cooling utility load requirements.

The key assumptions involved in the pinch analysis reflect the average temperature difference of the network (in this case a global ΔT of 20K is assumed) and the key assumptions surrounding the utility values, detailed in Table 3. The heat capacities of solids are assumed to be equal, with maximum heat recovery between inflow and outflow streams of the calciner allowing for the removal of high temperature heat required for solids preheating, this assumption is reasonable due to the lack of data available on solid-solid heat exchangers. Additionally, a total heat recovery is assumed in a heat exchanger connecting the steam preheat at calciner entrance and the steam separation.

Table 3 - Hot and Cold Utility Assumptions

Utility Name	Type	T	T	ΔT	h
		°C	°C	°C	kW/m²K
Concentrated Solar Power	Hot	1000	950	0.5	4.5
Medium Pressure Steam	Hot	700	400	0.5	4.5
Cold Water	Cold	10	15	0.5	2

3.2.5. Economic Analysis

The key cost considerations can be separated into: operational expenditure (OPEX); initial investment costs – capital expenditure (CAPEX); and revenue. This section details the key assumptions and calculations implemented into the economic analysis.

For calculation of annualised cost values an operation lifetime of 20 years and an operation capacity of 8000 hours/annum is assumed.

The NPV calculation is used as the key economic indicator of the process. It assesses the present value of inflows into the system versus the present value of outflows, accounting for the influence of interest rate (4.75% [109]) on the financial viability of the process. For this reason, the capital expenditure is annualised over the plant lifetime.

In order to ensure the economic calculations are performed using the same currency, the following conversion rates are assumed based on values provided by Xe.com on the 24th of May 2021 [110]:

$$€ = 1.22 * \$$$

$$€ = 0.86 * £$$

$$€ = 10.16 * SEK$$

3.2.5.1. Operational Expenditure (OPEX)

The operational costs associated with the model can be divided into two sections: utility costs and material costs.

The utility costs are divided into two key areas: reaction heat and process heating. The calciner reactor requires high temperature heat to meet the reaction temperature (925°C), for the purposes of this study this heat is assumed to be provided by a CSP plant, following data gathered in previous research by Castilla et. al. [109]. The data provided an average high temperature heat cost of 45 €/MWh_{th} [109], which is used within the economic calculations of this project.

Process heating energy flows are provided by a steam flow. The cost of this steam is calculated (Eq. 12), from the assumed electricity price (detailed in Section 3.2.5.3) and a basic steam cycle efficiency, to provide a steam price of 22.52 €/MWth. Process cooling loads utilise a general cooling water assumption based on the literature of approximately 0.036 €/MWh_{th}. [109]

$$C_{steam} = C_{elec}\eta_{steam} \qquad (Eq. 12)$$

These process heating costs are multiplied by the utility requirements estimated in the pinch analysis.

The operational material costs are dependent upon the cost of new material inflow (assumed at 10 €/tonne [109]), based on the make-up flow requirement (detailed in Section 3.2.3.), and the disposal cost of purge flows, assumed at 2,2 €/tonne.

Additionally, the reactor requires loading (the quantity of mass required to undertake one cycle), which has a corresponding minor annualised cost.

3.2.5.2. Capital Expenditure CAPEX)

The only CAPEX costs considered within the model are the costs of reactor construction, assuming, based on a previous study [109] that they represent 80% of the capital expenses. The reactor costs are calculated based on a cost function developed by Castilla et. al. [109]. It is important to note that since the cost equation is based on the thermal input or output of the reactor, it does not consider the variation in reactor sizing that would be required due to an increased circulation rate resulting from particle deactivation.

3.2.5.3. Revenue

The core sources of revenue considered within the model are associated with the energy sold from the carbonator output, and the savings resulting from carbon tax reductions should the system be connected to a plant emitting CO_2.

The energy output from the system is valued at the reverse conversion of plant efficiency detailed in Eq. 12, assuming a 100% steam raising efficiency, using a base electricity price of 40€/MW_{el}, [109].

The revenue from carbon capture is presented as revenue inflow. The revenue is estimated by calculating the cost of emission of the FG entering the carbonator, and subtracting from it the cost of emissions leaving the system. These costs are estimated by multiplying the carbon tax (70 €/tCO_2) by the annual CO_2 flow recovered (tCO_2/annum).

Storage streams are modelled within the process for certain sensitivity cases. The storage of solids at an intermediary stage corresponds to a subsequent storage of energy from the process, it is assumed that these solids are carbonated at a later point when energy demand from the system is higher. The stored solids therefore have the potential to shift the energy output of the system, corresponding to an increased sale price of energy out in a well-designed system. In order to take in to consideration the potential of load shifting, the potential energy stored within the solids is valued at the peak electricity price of 80 €/MW_{el} [109] at discharge.

3.3. Base Case

A base case is analysed considering a simple open-loop system, where the purge-split fraction within the 'PRGESPT' block is set to 1, i.e., all solids entering the system are circulated and then removed. This case can be considered a worst-case scenario in terms of material conservation for comparison with the results of the sensitivity analysis. Ten simulations were undertaken for this case, each of which involves an increase in calciner power capacity in stages of 100MW, from 100MW to 1GW.

The case considers an average particle activity of the single-cycled particles of 70 % within the carbonator for mass-flow calculation, this value is assumed based on the literature [87]. It should be noted that this is higher than the targeted activity of 60 % that is implemented within the sensitivity analysis (Section 3.4), as the value for repeated cycling can be set externally by the user. The difference between targeted activity in the base case and sensitivity analysis is to avoid a required purge flow fraction of one following multiple cycles of solid material.

The carbon-capture rate is set at 95 % in the base case. An ideal capture rate of X_{CO2} = 100% is not feasible in reality as it would result in extremely high solid flows and/or long residence times. [17]

The model outputs the mass and energy balances of the process for further analysis within the Excel spreadsheet, to allow the determination of the profitability of the system for different capacities.

3.4. Sensitivity Analysis

This section describes the two sensitivity analyses undertaken. The first sensitivity analysis involves the variation in the particle cycling within the system. The second sensitivity analysis involves the variation of the carbon capture rate, set within the 'CACO3FLO' Design-Spec block.

For each sensitivity analysis a series of cases are defined based on the varied values.

3.4.1. Analysis of particle cycling

The first sensitivity analysis reviews the impact of varying particle cycle numbers (N_{cyc}) for a set CO_2 capture rate and average particle activity of 0.6, with the make-up flow rate calculated according to the method detailed in Section 3.2.3.2 and the activity following each cycle extracted from [87]. This involves the recalculation of purge and corresponding make-up flow fractions for each simulation (according to Section 3.2.3.2). This series of cases should allow the determination of the optimal balance of higher disposal costs arising from low circulation rates versus reduced power outputs from the system as a result of increasing circulation of deactivated solids.

The increase in the number of cycles results in a greater circulation of inactive solids, accounted for in the model by adjusting the reaction conversion within the carbonator, detailed in Section 3.2.3.

For each case an increase in particle cycle number of 3 was selected, from 3 cycles within the system to 9. The reasoning behind this selection is due to the relatively small decrease in activity between particles as the cycle number increases beyond 9, demonstrated in [63], which would lead to similar results across further cases.

3.4.2. Analysis of carbon capture rate

The aim of this analysis is to determine the effect of varying carbon capture rates on storage flow rates exiting the STORSPLT block for fixed solid and FG inflows, and the subsequent impact on system sizing and economics. The comparison is undertaken for the base case and the best test case identified in Section 3.4.1 (a particle cycling number of 9).

The FGFLO Design-Spec block is modified to vary the split-fraction in STORSPLT to set the carbon capture rate, i.e., extracting solids from the cycle prior to conversion in the carbonator for CO_2 extraction and heat release. This differs from the base case, where the carbon capture rate was controlled by varying FG flow into the system. To achieve a particle cycling number of 9 a partial recirculation is required by means of a purge splitter with solids recirculation and outflow, the split fraction (detailed in Section 3.2.3.2) is modified to consider the solids flow removal in the storage as part of the required purge flow.

The FG flow values are input from the molar flow calculated in the base cases, the make-up (and hence internal) flow rate is maintained at the original values for the sensitivity cases.

The base case and previous sensitivity set assume a carbon capture rate of 0.95, in this sensitivity set this value is varied to 0.9, 0.8 and 0.7, for comparison. The cases studied in this sensitivity analysis are detailed in Table 4.

As the solids exiting the system are passing to storage, their load shifting potential is considered in economic calculations, with the heat stored being output at the upper electricity price of 80 €/MWh_{el}. The future revenue potential arising from the CC capability of the stored solids is not included in the economic calculation due to potential variation in carbon taxes and the potential for solids-transport and utilisation in a closed-loop system.

Table 4 - Carbon Capture Sensitivity Test Cases

Sensitivity Case	**Particle Cycle Number (N_{cyc})**	**Carbon Capture Rate (X_{CO2})**
Base case 1	1	0.95
Base case 2	9	0.95
1	1	0.9
2	1	0.8
3	1	0.7
4	9	0.9
5	9	0.8
6	9	0.7

4. Results and Discussion

This section presents the results obtained from the process modelling and economic analysis of the system. Results from the base case of an open-loop system are presented and analysed, following which the results of the selected cases are reviewed in the sensitivity analysis are detailed.

4.1. Base case

The results of the base case are collated in this section, this case shall be used as a benchmark for further comparison with the sensitivity analyses. Detailed values for the results generated in the Base Case are displayed in Appendix C – Detailed Results Base Case.

The variation in $CaCO_3$ feed rate into the calciner (t/h) as the calciner power input increases is displayed in Figure 9 for the base case. The graph displays an approximate increment in the flow rate requirement of 2.23 t/h/MW, following a linear trend which can be expected according to Equation 1, which relates calciner power input to molar flow of active carbonate.

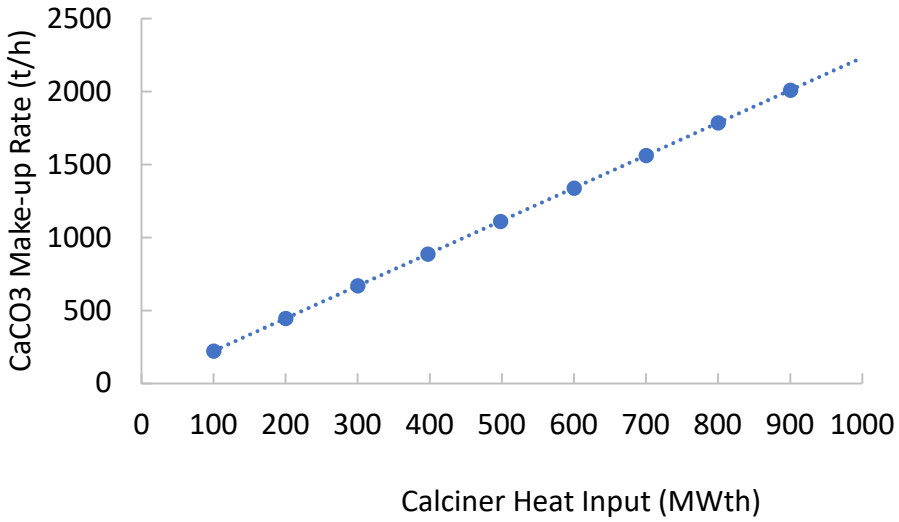

Figure 9 – Base case $CaCO_3$ make-up flow requirement at different heat inputs to the calciner

The carbonator heat output is shown in Figure 10 as a function of calciner power for the base case across the ten simulations. The carbonator is set to convert 70 % of the CaO inflow in the base case, which should therefore result in a carbonator power output value approximately 70 % of the level of calciner input according to the reversible carbonation/calcination reaction detailed in Eq. 1. The residual 30% of calciner power input is retained within the unconverted solid, which is discharged without release. A linear trend can be noted as the calciner size increases, as can be predicted from the linear pattern observed in Figure 9. The increase in solid flows within the system corresponds to an increase in both calciner input requirement and carbonator output.

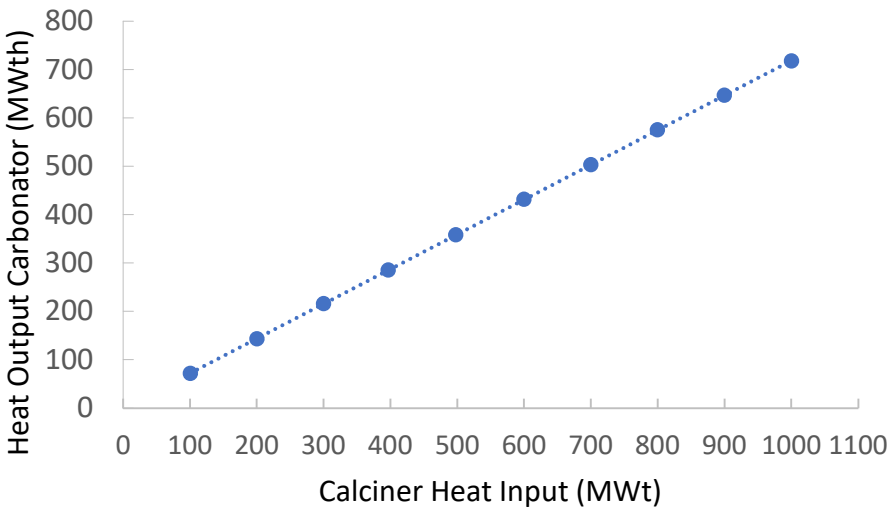

Figure 10 - Base Case carbonator heat outputs for varying calciner heat inputs

Figure 11 – Base case NPV estimation displays the NPV estimation for the CaL process. A non-linear trend is observed, in this case the trend is negative with the estimated NPV of the system decreasing for each step-up in size between simulations, indicating that an investment in the plant will prove unprofitable over the expected lifetime. This negative trend is highly dependent on the economic assumptions input into the model. The non-linear trend of the NPV is related to the calculation of reactor costs, which become more economical at scale. The reactor costs are a factor of 10 smaller than the difference between the OPEX and revenue of this system, as such the non-linear trend is not easily identified from the graph. For a system with a calciner size of 100 MW, the NPV is approximately -30 M€, decreasing to only -261 M€ at GW scale.

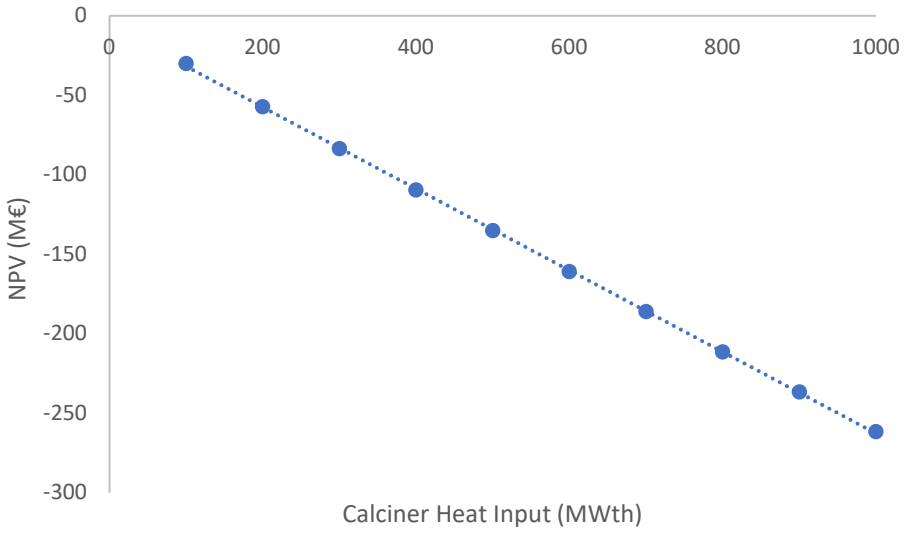

Figure 11 – Base case NPV estimation at different calciner heat inputs

4.2. Sensitivity analysis

This section presents and discusses the results of the two sensitivity analyses, with comparison to the base case.

4.2.1. Particle cycling sensitivity

The results of the particle cycling sensitivity analysis, outlined in Section 3.4.1, are described and discussed in this section. In this section the varying number of cycles of solid material prior to total system discharge is represented by N_{cyc}.

Figure 12 displays the varying heat output in the carbonator for the three different values of N_{cyc} (3, 6 & 9). Evidently, the carbonator power output is similar for the three values of particle cycling number, ranging from 63 MW for a calciner power of 100MW to 634 MW for a calciner power of 1GW as a result of the similar value of particle activity set externally. The carbonator power output is significantly higher (~16% increase) for the base case (N_{cyc}=1) for each simulation. Similar to the findings of the base case, the carbonator power progresses linearly with increasing calciner power input.

The similarity in carbonator power output across the three sensitivity cases of higher cycle number is related to the targeted particle activity of 60%, with adjusted make-up and recirculation flows to ensure similar activity, across the three cases. It can be noted in Figure 12 that the carbonator output values are slightly above the expected value (5-10% higher across the three cases), this discrepancy can be associated with minor calculation errors in the make-up flow rate requirements.

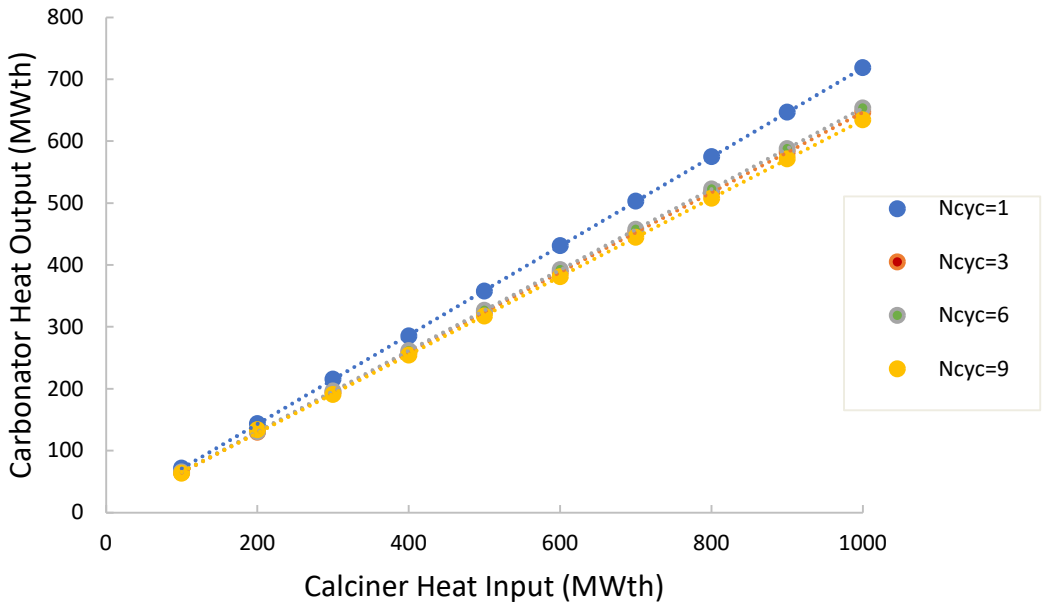

Figure 12 - Particle Cycling Sensitivity Analysis Calciner Power v.s. Carbonator Output

The variation in make-up flow rate is detailed in Figure 13 across the base case (N_{cyc}=1) and three particle cycle rate variation cases (N_{cyc}= 3, 6 & 9). The graph indicates a linear pattern across all three cases. The base case (N_{cyc}=1) has the highest material requirement, closely followed by a N_{cyc}=3, with a make-up flow requirement of approximately 2.18 t/h/MW. The third sensitivity case evidently has the lowest make-up material flow requirement of 1.69 t/h/MW, a 24.2% decrease in flow requirement compared to the base case – N_{cyc}=1.

This result can be explained as all three sensitivity cases have relatively high purge flow rates (between 27 and 40% of recirculation flow), with N_{cyc}=3 having the lowest fractional purge and N_{cyc}=9 the highest. However, as the goal of the first case (N_{cyc}=3) is to cycle the system three times before fully purging the system (compared to nine circulations before purging the system in case 3), the average make-up flow requirement in the first case is equal to the calculated purge flow plus one third of the recirculation flow. Due to the addition of the total purge the make-up mass flow rate required is significantly higher than in test case 3 (N_{cyc}=9, which has a higher purge fraction, however a lower average make-up requirement when system clearing is considered).

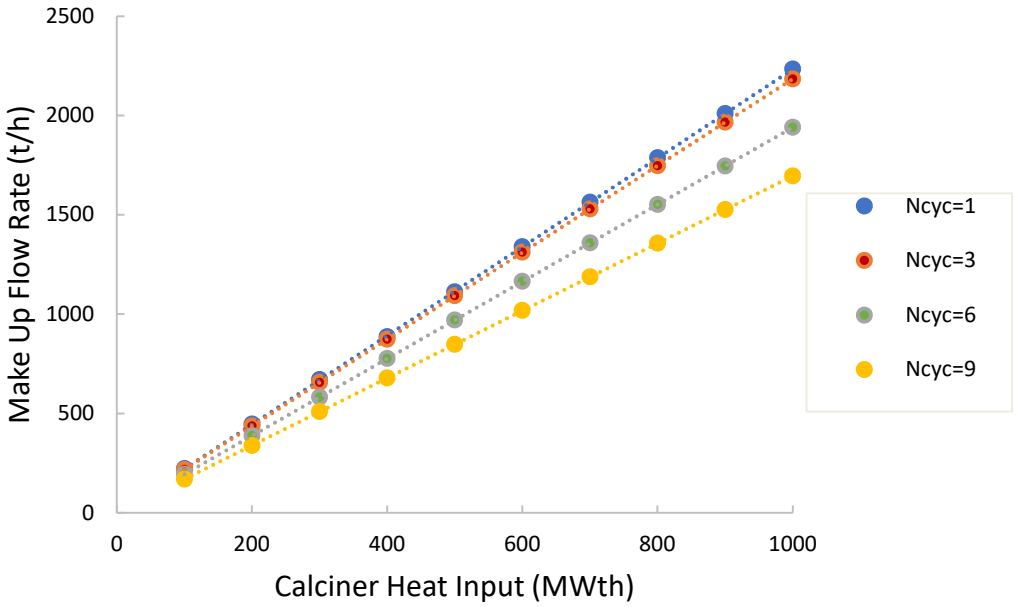

Figure 13 - Calciner Heat Input (MWth) v.s. Make-up Flow-rate (t/h) for different particle cycling numbers within the system

Figure 14 shows the variation in CAPEX for the three sensitivity cases (N_{cyc}=3, 6 & 9) compared with the base case (N_{cyc}=1), annualised across the plants lifetime of 20 years. The results for this variable are relatively similar across all four cases, with N_{cyc}=1 providing the highest CAPEX, and N_{cyc}=9 the lowest. In this case the results tend towards a maximum, with a decreasing gradient as calciner power rises, however the gradient change is sufficiently small that the maximum will not be reached within the reasonable operation of a plant.

The non-linear trend in CAPEX results from the equations used in calculation of reactor costs [109]. The calciner costing function is non-linear as a result of the inclusion of a factor of $(\dot{Q}_{input})$^0.67, a similar costing function is included in the carbonator costing, with the carbonator power similarly providing a non-linear trend as a result of being multiplied by a factor of $(\dot{Q}_{output})$^0.67. Therefore, an increase in calciner power, and subsequently the carbonator power (Figure 12 - Particle Cycling Sensitivity Analysis Calciner Power v.s. Carbonator Output) does not lead to a proportional increase in capital expenditure. Further to this, the calciner power dominates the capital expenditure, given the current system of equations used, due to its higher power input compared to carbonator output, as mentioned above this is not entirely accurate as the volumetric sizing of both reactors is not considered within the capital expenditure calculation, and will be larger than assumed due to the circulation of deactivated solids.

This result is to be expected based upon the economic calculations detailed in Section 3.2.5. However, it is important to consider that these calculations do not take into account the variation in volumetric capacity of carbonator and calciner reactors that would be required for the handling of increased solids flow resulting from particle deactivation. This would likely make case 3 less profitable.

Additionally, the model does not consider heat exchanger costings, which once again proves higher for the cases with a greater purge split-fraction as the increased solids flow exiting the system requires heat exchange with the incoming make-up flow, resulting in increased heat exchanger area requirement. The increased mass flows required for higher quantities of deactivated particles results in greater demands on material transportation systems, subsequently increasing their capital expenditure.

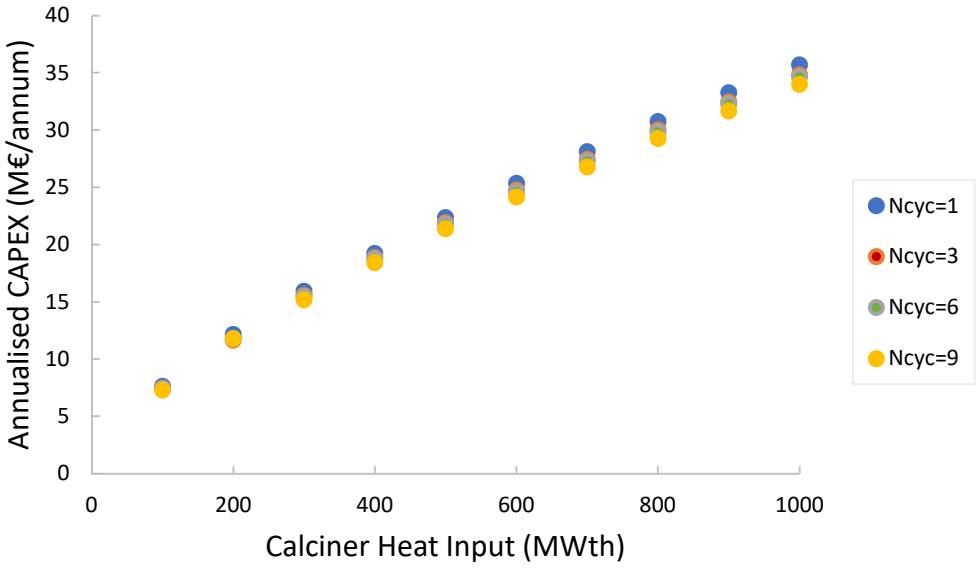

Figure 14 – Variation in annualised CAPEX across plant lifetime of 20 years with calciner heat input for varying particle cycling numbers

The impact of varying N_{cyc} on the FG flow rate requirement is shown in Figure 15. Again, the simulations follow a linear increase as the calciner power increases. The FG flow rate into the system is approximately 13% higher for N_{cyc}=1 than the three sensitivity cases (N_{cyc}=3, 6 & 9), which remain relatively equal across each simulation. Of the sensitivity cases, N_{cyc}=6 has the highest FG flow rate into the calciner (3.85 t/h/MW) and N_{cyc}=3 the lowest (3.73 t/h/MW).

The similarity in FG flows into the system is to be expected, with both calciner power and particle activity being set resulting in a similar set flow rate of active solids into the carbonator for the three sensitivity cases. The active solids can only react with a set quantity of FG, as such the flow rate of FG should be approximately the same for the three cases. The increase in FG flow rate in the base case (N_{cyc}=1) can be associated with the increase in particle activity and therefore increase of reactive solids present within the carbonator, allowing a greater FG flow.

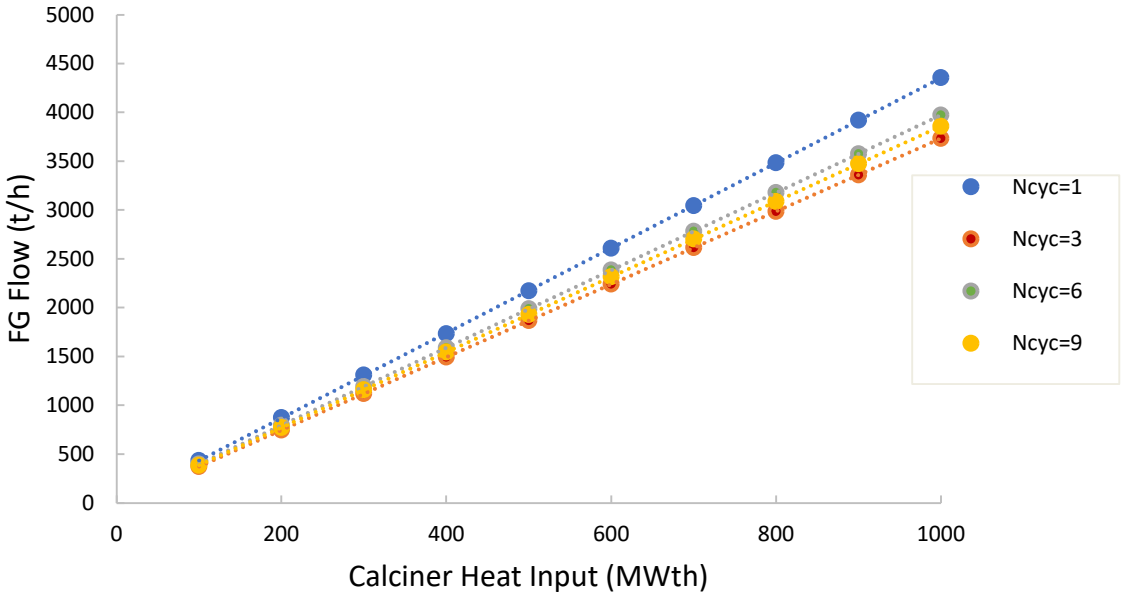

Figure 15 - Particle Cycling Sensitivity Analysis Calciner Power v.s. FG Flow Rate

Figure 16 displays a non-linear downward trend in NPV across the 10 simulations for all four analysed test cases. Sensitivity case 3 (N_{cyc} = 9) can be identified as the most profitable case, with the base case (N_{cyc}=1) and sensitivity case 1 (N_{cyc} = 3) displaying similarly low values, whilst sensitivity case 2 (N_{cyc} = 6) displays the economic results approximately in the centre of the results. The disparity between cases becomes more evident as calciner power increases.

As a result of the key economic assumptions made (Section 3.2.5) surrounding carbon taxes, electricity and material costs, the studied cases prove to be unprofitable, with the NPV becoming increasingly negative non-linearly as is expected from the CAPEX, carbonator power output and FG flow-rate results detailed above.

The revenue and CAPEX results of the sensitivity cases prove to be approximately equal. With the reactor sizes being similar across the three cases, and the maintaining of the particle activity at 0.6 resulting in similar power outputs and carbon capture quantities, however there is a variation in the operational costs resulting from the varying make-up and purge flow requirements, indicated in Figure 13.

Sensitivity case 1 (N_{cyc}=3) displays the poorest economic potential of the sensitivity cases, with the high make-up flow requirement (and associated high purge flow with high disposal costs) being 12 and 29% higher than case 2 (N_{cyc}=6) and 3 (N_{cyc}=9) respectively, and only slightly lower (~2%) in comparison to the base case. However, the particle activity is maintained at a lower level than the base case, resulting in lower Carbonator Power Output (Figure 12) and lower FG flow rates, with subsequently reduced CC potential, both of which result in lower revenue than in the base case. The difference in NPV between the cases with total system discharge (N_{cyc}=1) and discharge every 3 cycles (N_{cyc}=3) is minor.

Sensitivity case 3 (N_{cyc} = 9) is shown to be the most profitable of the four cases (including the base case) across the ten simulations. The lower total disposal rate required in this case (detailed in Section 3.2.2.2.2.) results in a substantially lower OPEX, for similar revenue and CAPEX to the other sensitivity cases.

It should be noted that the comparative profitability is highly dependent on the cost of material inflow (10 €/t) and disposal (2.2 €/t), the price at which heat is bought and sold and the carbon tax (70 €/t). It can be projected that an increase in carbon-tax price or the price of heat sold would improve the relative potential of the base case versus the sensitivity cases. Meanwhile an increase in the cost of material and/or its disposal would improve the relative profitability of sensitivity cases 2 and 3, due to their lower feed requirement.

The increase in NPV with increased solids cycling (N_{cyc} = 9 proving the most profitable) implies that increasing the solids cycling should further improve the profitability of the system, this result should be examined further.

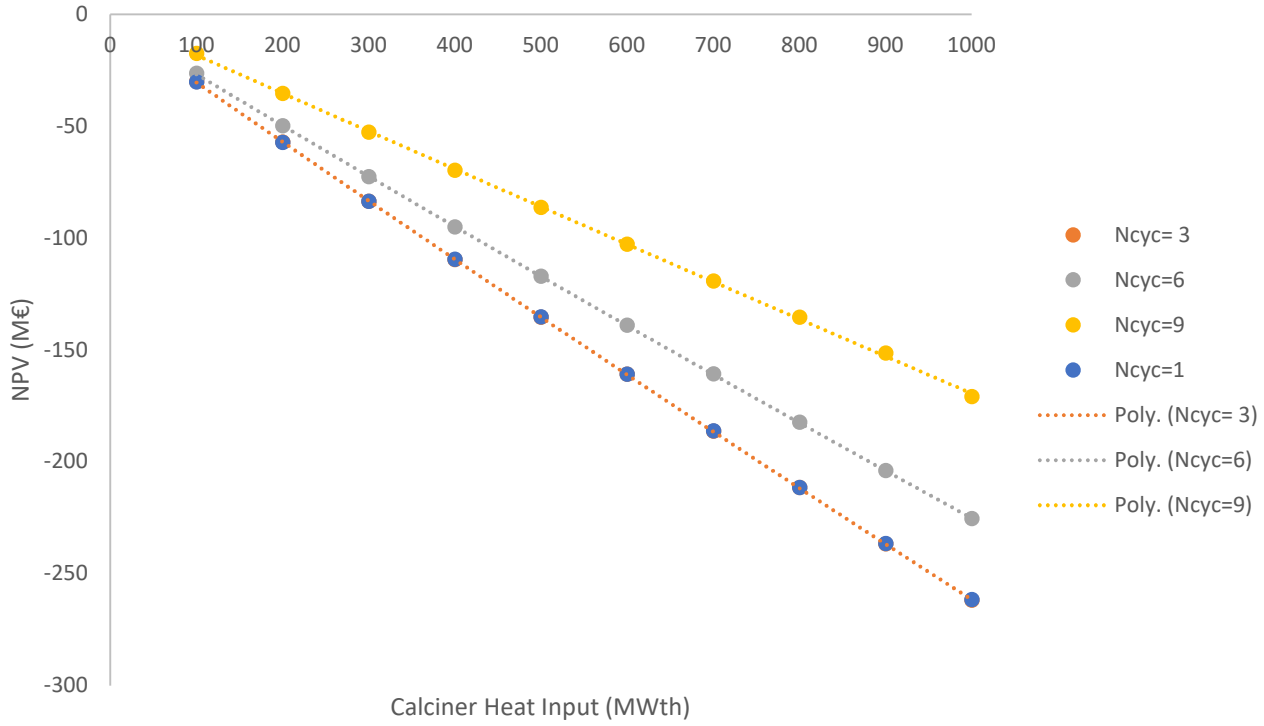

Figure 16 - Particle Cycling Sensitivity Analysis comparison of NPV of different cases across varying calciner heat inputs

4.2.2. Carbon capture sensitivity

This section presents and discusses the results of the sensitivity analysis detailed in Section 3.2.4., reviewing the effect of varying carbon capture rates (X_{CO2}) on the techno-economic balance of the system.

The impacts of varying carbon capture rates on carbonator power output are displayed in Figure 17 and Figure 18, for both one and nine particle cycles within the system respectively.

Figure 17 displays the impact of varying calciner power on the carbonator power output for different carbon capture rates, considering a particle cycling number of one. The base case (X_{CO2}=0.95) displays the highest carbonator power output, and sensitivity case 3 (X_{CO2}=0.7) the lowest.

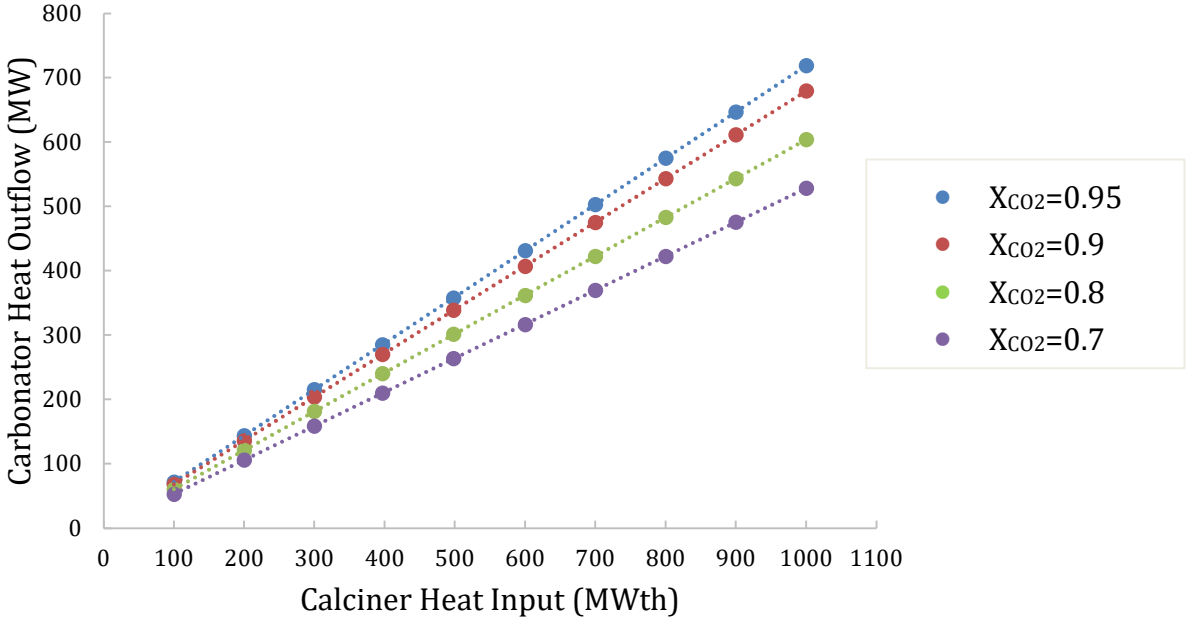

Figure 17 - Carbon Capture Sensitivity Analysis - Impact of Capture Rate on Carbonator Heat Output for a particle cycle number of 1

The range of sensitivity cases analysed for the higher particle cycling number (N_{cyc}) of 9 is shown in Figure 18, demonstrating the impact of varying calciner power on the carbonator power output for different carbon capture rates. The carbonator power increases linearly with increasing calciner power input, with the base case (X_{CO2}=0.95) displaying the highest power output and sensitivity case 3 (X_{CO2}=0.7) the lowest.

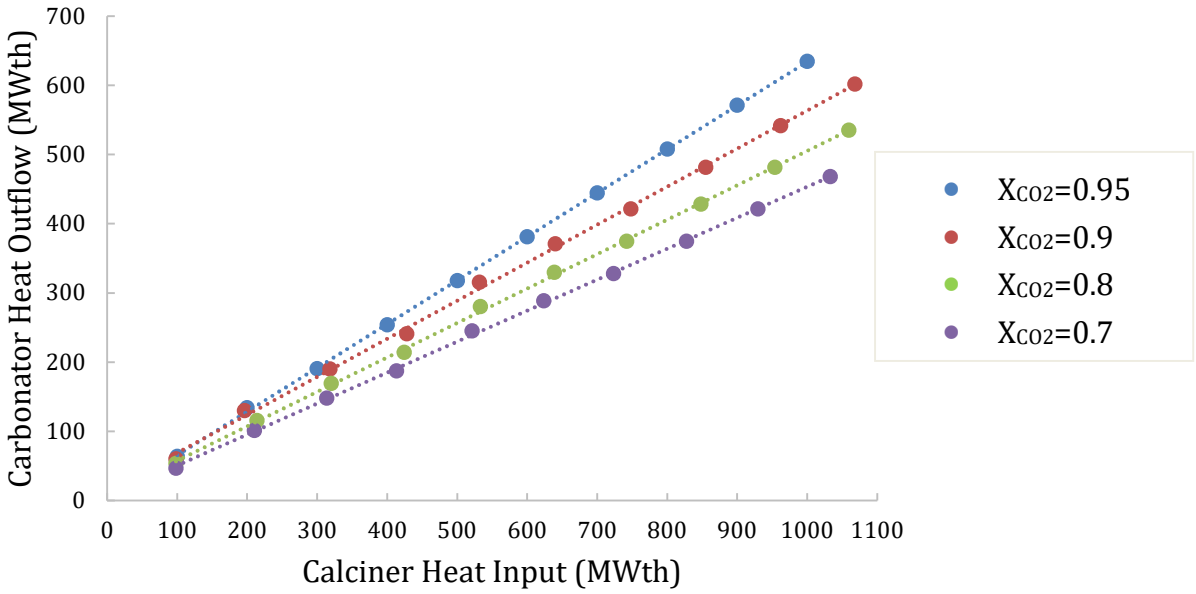

Figure 18 - Carbon Capture Sensitivity Analysis - Impact of Capture Rate on Carbonator Heat Output for a particle cycle number of 9

Figure 17 and Figure 18 exhibit slightly different gradients for the four tested cases. The percentage change in carbonator power between the different test cases remains constant in Figure 17, whereas Figure 18 displays some deviation from this pattern, with the base case (X_{CO2}=0.95) displaying a sharper relative rise in carbonator power than the other carbon capture rates, which indicates some variation in carbonator power increase with calciner power increase for different particle cycle numbers.

The rise in carbonator power with carbon capture rate, presented in Figure 17, is directly related to the increase in reaction extent for a fixed FG flow as a greater quantity of carbon is being reacted with the solids inflow. For sensitivity case 3 (X_{CO2}=0.7), the lower capture rate results in less solids reacting with the FG, and hence less heat is output.

A similar relationship is displayed in Figure 18, with increased power output for greater carbon capture rates. However, a marginally different ratio between the different power outputs of the various cases can be observed. This is associated with the aforementioned modelling inaccuracies.

The following figures detail the impact of varying carbon capture rate upon storage flows exiting the calciner as carbon capture rate varies. A series of cases are presented in
Figure 19 for a particle cycling number of 1, similarly Figure 20 presents a series of cases for a particle cycling number of 9. As the storage flow is equal to zero in the base case for both particle cycle numbers (N_{cyc}=1 & 9) , these results are not plotted.

From
Figure 19, sensitivity case 3 (X_{CO2}=0.7) can be identified as requiring the highest storage flow rates, with a mass flow rate of approximately 350 t/h being extracted from the carbonator at the GW scale. Sensitivity case 1 (X_{CO2}=0.9) has the lowest storage flow rate (~50 t/h at the GW scale).

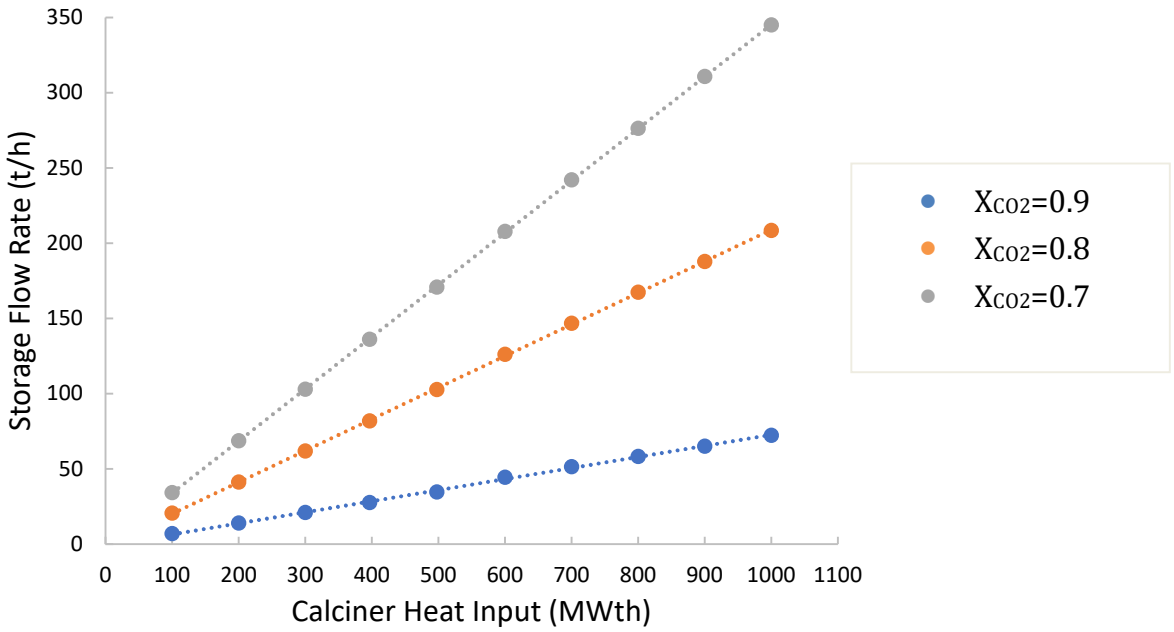

Figure 19 - Carbon Capture Sensitivity - impact of capture rate on storage flow rates at calciner exit for a particle cycle number of 1

Figure 20 displays a similar pattern to
Figure 19 Figure 19. For a N_{cyc}=9 storage flow rates rise with calciner power. Similarly, lower carbon capture rates require higher storage flows at calciner output for constant FG flows.

It should be noted that the storage flow rates are substantially higher in Figure 20 (N_{cyc} =9) than Figure 19 (N_{cyc} =1).

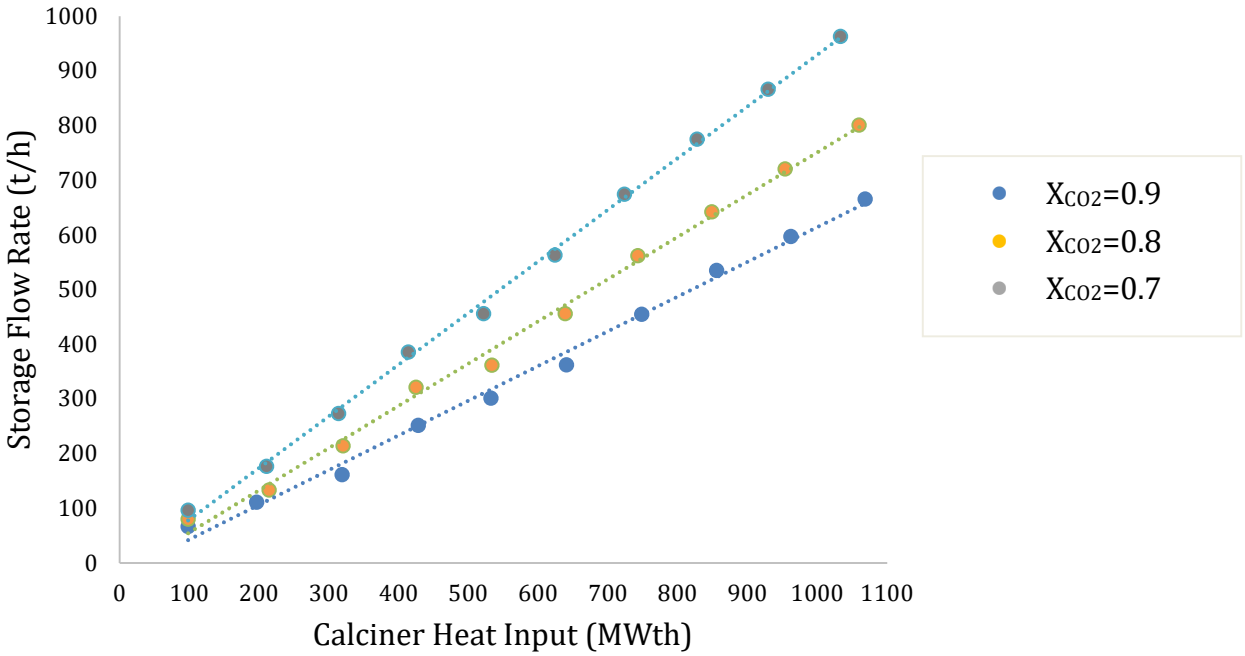

Figure 20 - Carbon Capture Sensitivity - impact of capture rate on storage flow rates at calciner exit for a particle cycle number of 9

For a N_{cyc}= 1 (Figure 19) the gradient of the storage flow rate rise is constant for each capture rate. The higher storage flow rate with decreased capture rate can be associated with lower solids flow requirement for reacting a decreased quantity of carbon in the fixed FG flow.

A similar pattern is displayed in Figure 20, with larger storage flow rates for low capture rates as a result of decreased reaction extent within the carbonator. The mass flow rates displayed in Figure 20 are substantially higher (approximately three times larger) than those in Figure 19 as a result of the increased internal mass flow rates for the higher particle cycle number set. The cycling of deactivated particles within the system (approximately 40% of all particles cycling) and the higher flow rate required within the system for particles with lower activity to produce equivalent calciner and carbonator outputs results in the higher flow rates identified.

As the storage flow is a fraction of the required flow into the carbonator, the storage flow rate increases for higher circulation rates typical for increasing N_{cyc}. These higher storage flow rates have a knock-on energy balance implication within the system, removing energy from the system that would be released within the carbonator in a continual cycle, in addition to requiring increased heat exchanger area to reduce their temperature to ambient storage conditions.

The impact of varying calciner power input on the annualised net income of the process is shown for both N_{cyc}=1 (Figure 21) and 9 (Figure 22).

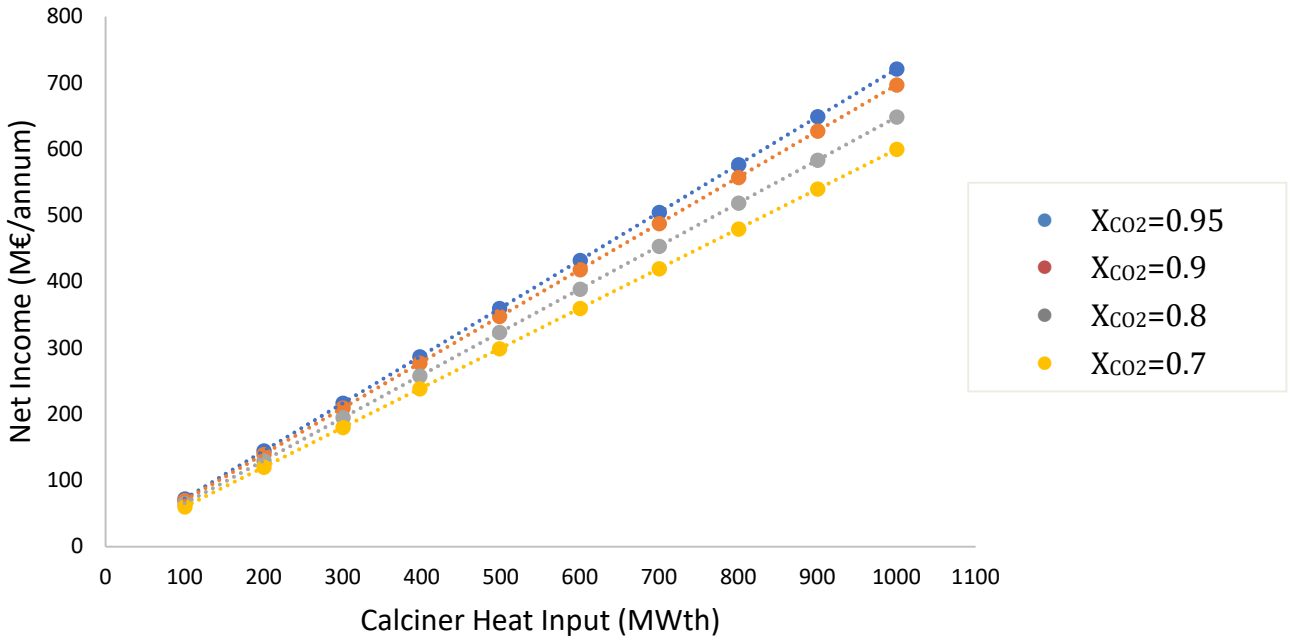

Figure 21 - Carbon Capture Sensitivity - Impact of capture rate on process net income for a particle cycle number of one as calciner heat input varies

Figure 21 outlines the variation in annualised net income across the range of calciner power inputs. Evidently the base case (X_{CO2}=0.95) has the highest net income, with sensitivity case 3 (X_{CO2}=0.7) the lowest. It should be noted that the ratio of net incomes between the different cases remains constant across the 10 simulations.

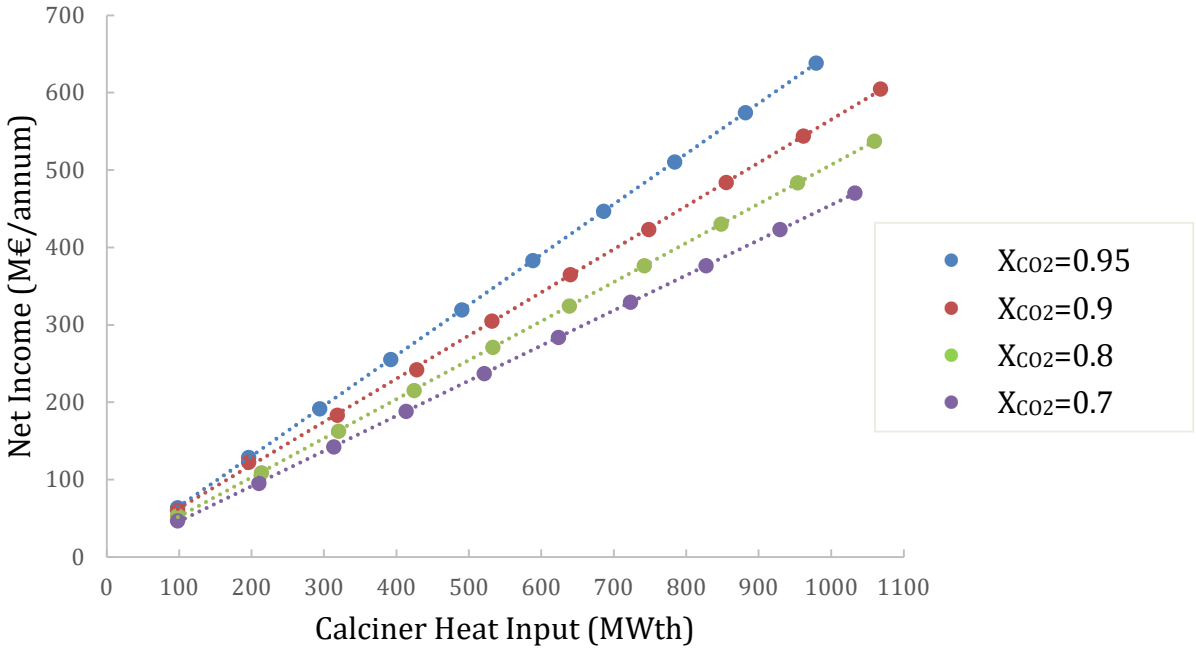

Figure 22- Carbon Capture Sensitivity - Impact of capture rate on process net income for a particle cycle number of nine as calciner heat input varies

Figure 22 displays the impact of carbon capture rate on the annualised net income of the process for N_{cyc}=9. Similar to Figure 21, the base case (X_{CO2}=0.95) presents the highest net income, with sensitivity case 3 (X_{CO2}=0.7) the lowest across the range of calciner power inputs.

There is a greater disparity between the different cases, in terms of net income as the calciner power increases, in Figure 22 than Figure 21. For N_{cyc}=9 the net income is substantially higher for the base case (X_{CO2}=0.95) than the other cases as calciner power rises. It can be noted that the net income of all cases is lower for a higher N_{cyc} (Figure 22) than a cycle number of 1, with the annualised net income of the base case dropping from 710 M€/annum to 640 M€/annum at 1GW between the two analyses.

The higher net income demonstrated by the base case (X_{CO2}=0.95) for N_{cyc}=1 demonstrates the dominant impact of the carbon tax and carbonator power output on the overall income compared to the value of heat recovery from stored solids. For a higher capture rate, the saving associated with reduced carbon tax will be higher, as will the income from heat sold due to the increased carbonator power detailed in Section 4.2.1. However, the higher carbon capture rate cases demonstrate decreased potential for heat recovery from solids storage during periods where output price is higher.

A slightly different pattern is displayed for a higher N_{cyc} in Figure 22, with the relative net income of the system increasing more rapidly with calciner size for higher capture rates than lower ones. This can be explained by the varying economic balance as cycle number increases, and particle activity decreases. The Aspen+ model takes into consideration particle deactivation on the ninth cycle within the carbonator reactor, therefore solids separated prior to this reactor (i.e. at the post-calciner storage splitter) will have a higher average particle activity than the targeted 60%. Therefore, the net income from storage discharge will be higher, however the overall average particle activity within the system will be lower as a result of increased flows of active particles (particularly those entering from the make-up stream) exiting the system prior to carbonation.

The impact of modifying the carbon capture rate on the NPV of the system for both one solids-cycle (N_{cyc}=1) through the reactors and nine cycles (N_{cyc}=9) are detailed in both Figure 23 and Figure 24 respectively.

Figure 23 displays the variation in NPV with calciner power of a system cycling solid particles one time prior to removal for four different carbon capture rates. A non-linear reduction in NPV for increasing calciner power is displayed in all four cases, with the base case (X_{CO2}=0.95) proving the most profitable of the four cases and sensitivity case 3 (X_{CO2}=0.7) proving to be the least profitable.

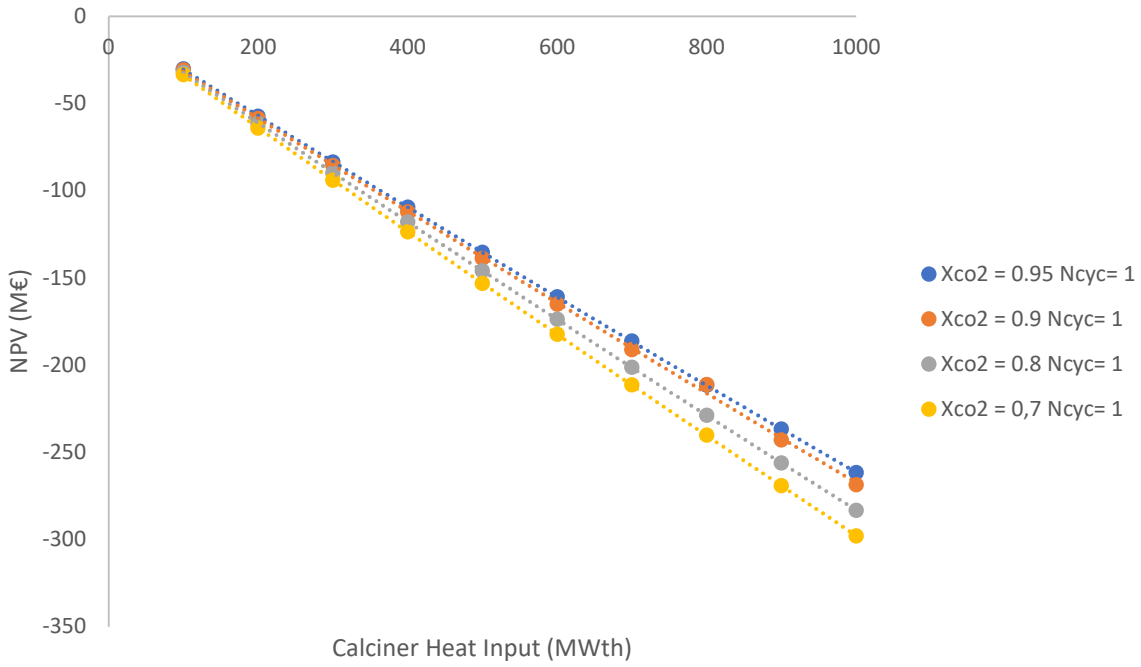

Figure 23 - Carbon Capture Sensitivity Analysis - Impact of Capture Rate on System NPV (Particle Cycle = 1)

Figure 24 displays the variation in annualised NPV with calciner power of a system cycling solid particles nine times (N_{cyc}=9) prior to removal for four different carbon capture rates. All four cases exhibit a non-linear decrease in profitability as the calciner power increases, indicating that the current economic considerations produce a non-profitable project.

Sensitivity case 1 (X_{CO2}=0.9) proves to be the most profitable case at all calciner powers, and sensitivity case 3 (X_{CO2}=0.7) the least. Initially, the base case (X_{CO2}=0.95) proves to be more profitable than sensitivity case 2 (X_{CO2}=0.8), however, as the calciner power increases, the base case NPV decreases more drastically and sensitivity case 2 proves to be more economically viable.

Similar to the results identified in Section 4.2.1. a particle cycle number of nine proves more profitable than a cycle number of one for all test cases.

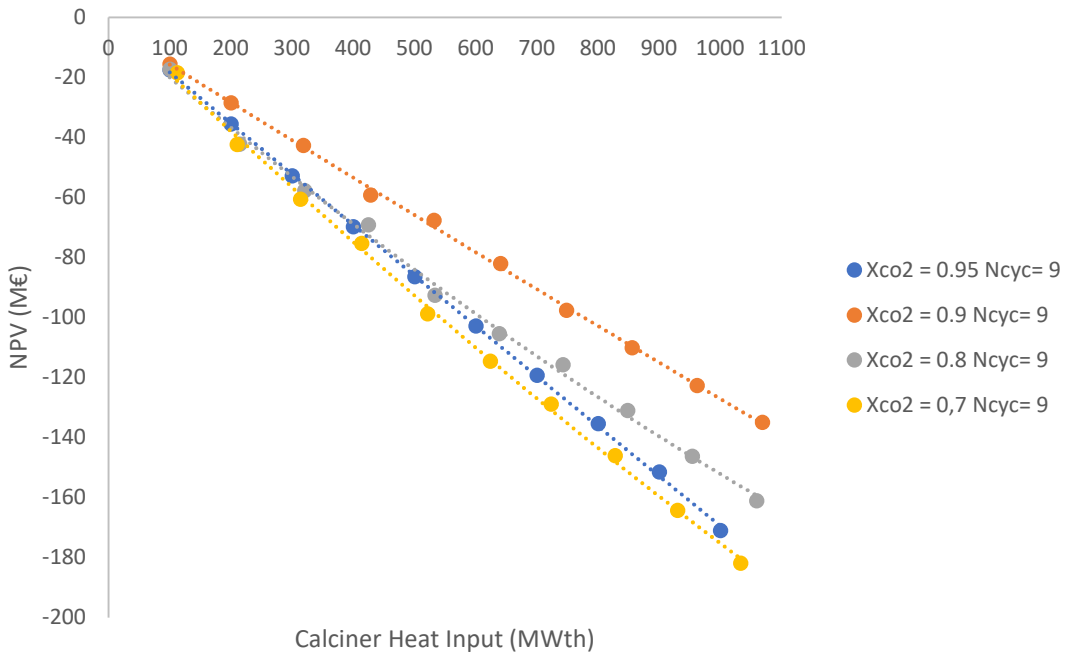

Figure 24 - Carbon Capture Sensitivity Analysis - Impact of Capture Rate on System NPV (Particle Cycle = 9)

For N_{cyc}=1 the non-linear decrease in NPV across all four cases with rising carbonator power can be associated with the same trends detailed in Section 4.2.1. The decrease in NPV as capture rate decreases illustrates the dominance of income associated with savings in carbon tax (70 €/t) and energy recovery from immediate discharge over the income flows related to discharge from storage and the higher costs associated with disposal from systems not storing solids and the higher CAPEX resulting from increased carbonator sizing. As the FG inflow remains constant and the solids make-up flow is fixed for all four cases, there is no impact of costs associated with heating utilities and make-up flow material costs.

As N_{cyc} increases a different pattern is displayed, with the base case (X_{CO2}=0.95) proving more profitable at lower power outputs than sensitivity case 2 (X_{CO2}=0.8). The base case then subsequently experiences a more rapid decrease in profitability than sensitivity case 2 and the lines intersect, with X_{CO2}=0.8 proving more profitable at higher power outputs. This change can be associated with the balance between income from storage (which is not required for the base case), and other revenue and cost flows. Income from storage has a more notable effect for higher material flow rates and calciner heat flows, therefore resulting in a different profitability pattern from a system which does not include storage as a variable. A similar pattern is observed for a particle cycle of one, however this impact is less noticeable due to the higher activity and subsequent carbonator power output.

There is some inaccuracy in the calculations associated with the capital expenditure relating to reactor sizing. As detailed Section 4.2.1., for the other sensitivity analysis, the particle deactivation results in increased reactor size, and subsequently increased costs which are not considered within the cost calculation. The consideration of varying reactor size would increase the profitability of lower capture rate cases. Additionally, the solids-storage cost is not included within the economic calculation, this would play a considerable impact, and would notably increase the operational expenditure of lower capture rate cases, where solids are stored at a greater rate. For cases assessing the impact of a particle size equal to one, the

base case (X_{CO2}=0.95) proves more profitable, in the case of higher particle cycle number, a lower carbon capture rate proves more

4.2.3. Economic considerations

The four graphs of NPV presented within this report (Figure 11, Figure 16, Figure 23, Figure 24) display solely negative results for the given economic considerations. This section will briefly demonstrate the impact of the economic considerations used in this report on the system economics by presenting one test case with increased revenue flows.

In the aforementioned figures the carbon tax price is set at 70 €/tCO_2. Figure 25 displays a comparison of NPV across the range of calciner heat inputs for the base case (N_{cyc}=1, X_{CO2}=0.95), when the carbon tax is set at 70 and 100 €/tCO_2 respectively (based on predicted future carbon pries). This shift in trend of NPV from negative to positive with increasing carbon tax demonstrates the potential of the systems to produce profit dependent upon the economic situation of the plant. It can be projected that this rise in NPV would be even larger for the more profitable cases identifies in the sensitivity analysis. In the previous graphs, the non-linear impact of CAPEX values resulted in a flattening of the curve – i.e., the ratio of NPV to MWage became less negative, with a reducing cost per MW of the reactors. When the carbon tax is increased, and a subsequent rise in NPV to positive values is observed, the non-linear impact of the CAPEX costs results in the NPV gradient becoming gradually more and more positive, with the NPV at the 100 MW scale being approximately 18.3 M€, rising to 223 M€ at GW scale.

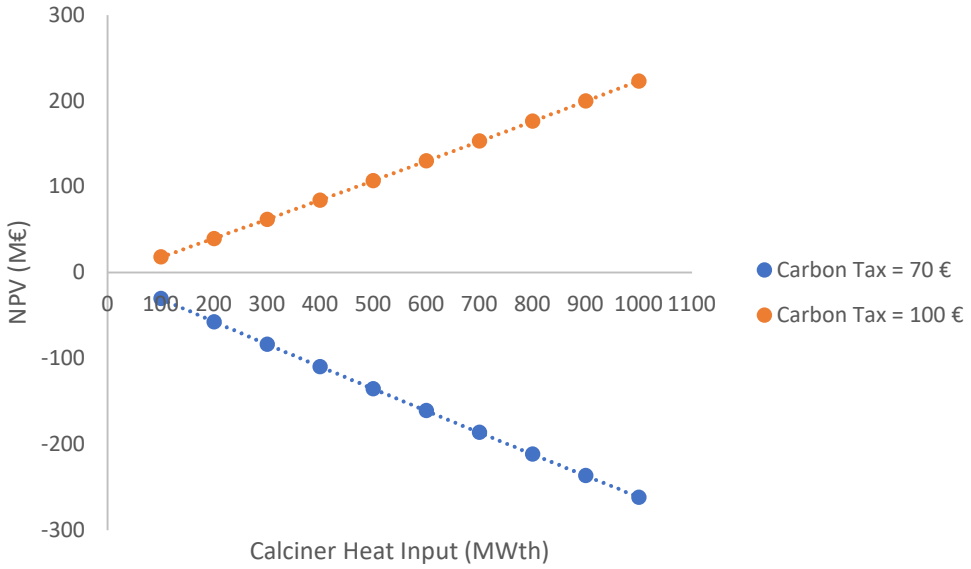

Figure 25 - Comparison of NPV for varying carbon tax levels across a range of calciner heat inputs

4.3. General Discussion and Limitations

The results and discussion, detailed in Sections 4.1 and 4.2, provide a technoeconomic analysis of a calcium looping system for combined CCS and TCES applications. For the tested cases, a particle cycle number of 9 can be identified as the best case for varying capture rates in terms of system economics for the specified input assumptions.

However, there are several key inputs which have not been considered in the model, which would likely have a notable impact upon the results.

Firstly, the impact of steam fluidisation in the calciner has not been incorporated into the activity assumptions, steam flows have been demonstrated to display attrition effects on the particles, leading to particle disintegration. This disintegration can lead to increased mass losses and reduced particle activity. These effects where not considered due to conflicting information within the literature on the extent of the impact. [85] Further, the effect of steam on particle activity is only considered as a general assumption, this could be better modelled by means of an series of intermediary reactors to define the surface reactions that particles undergo during steam regeneration. [63]

Secondly, the impact of reaction kinetics on the process was not considered within the model, with approximations over reaction extent and residence times based on findings within the literature. The impact of reaction kinetics on reactor sizing would have a major influence over the economic viability of the project, and would likely decrease the profitability of cases involving reduced particle activity more notably than in the singular cycle case.

As the process modelling software provides a steady state model, the range of cases considered for varying N_{cyc} only reflects the economic calculation on the final circulation through the system, using this value as an average across the full circulation. In reality simulations should be undertaken for each cycle number with the given make-up flow rate, determining the mass, energy and economic flows for each system cycle, to be averaged before input into the final economic calculations. This would likely result in larger carbonator power output requirement, and subsequent cost.

There are numerous cost considerations not included within the model. Notably, several capital expenditure costs are not included within the economic analysis, including the cost of solid-separators, the CO_2 compression train and heat exchangers (due to the lack of information regarding solid-solid heat exchanger sizing and design). Additionally, the cost of material conveying and storage of solids and CO_2 are not factored in to the economic calculation as specific process design is not included in this analysis. These considerations would likely decrease the profitability and NPV of all cases reviewed within the project.

Further limitations in the economic analysis relate to the consideration of NPV variations with changes to the economic assumptions. It can be inferred that NPV patterns would likely vary with changes to the economic inputs, including: power input and output price; limestone costs; disposal cost; and the upper power output price vary. These variations would be most interesting for the second sensitivity analysis case (varying X_{CO2}) at N_{cyc}=9, with the intersection between sensitivity cases under the current economic assumptions. Altering the gradient of the NPV vs Calciner Power curve (Figure 24) by varying the economic inputs would lead to the identification of a different optimal value of X_{CO2} for different calciner heat flows.

5. Conclusion

This thesis provides a techno-economic analysis of a calcium looping process for combined TCES-CCS applications. A detailed process model has been developed using Aspen+ to provide insight into the mass and energy balances of the system. The study accounts for the impact of variation in both the number of cycles of the solid material within the system and the carbon capture rate. Comprehensive economic calculations have been undertaken to compare the financial viability of different test cases.

For the tested cases, the process modelling and economic evaluation allowed the identification of 9 cycles of the carbonate material as a best-case scenario from the series of runs undertaken, given the specific assumptions made within the project. In order to maintain the targeted particle activity of 60% a make-up flow should be maintained at 38.75% of the internal mass flow requirement, set by the power requirements within the reactor. Although not shown in this work, the trends observed indicate that increasing the number of solid cycles within the system will result in further improvements in process economics, with the high discharge rates at lower cycle numbers bringing a major cost implication to the profitability of the system. The deactivation data presented by Champagne et. al. [63] indicates the activity of particles does not reduce greatly as the cycle number increases. It can be projected that the make-up flow rate requirements would not increase significantly for higher cycle numbers, whilst requiring a reduced total mass purge of the system as full discharge is less frequent.

The results of this work show the economically optimal carbon capture rate is dependent upon the particle cycle number used. Of the studied cases in this thesis, a carbon capture rate of 90 % provides the best results in terms of NPV for a particle cycle number of 9, whereas a capture rate of 95 % is preferable for a particle cycle number of one. This trend is linked to the savings in solids-disposal costs that can be achieved from increased solids-storage prior to purge, this saving is larger in cases of increased particle cycling as the reduced activity results in greater mass flow requirements – the impact of which would be less significant should storage costs be considered. These trends highlight the importance of balancing the operational costs, which will vary according to the system mass flows, with the incomes from power output and carbon tax reductions.

The project sought to define a general model to demonstrate trends across different test cases, providing accurate calculations of mass, energy and economic balances within the system. Given the current economic inputs the studied cases prove unprofitable (with a negative NPV output in all simulations), the profitability of these cases would be improved should the parameters involved in economic calculations modify for different scenarios, as would be the case in practical applications. The key inputs which would increase the profitability of the process would be rising carbon taxes and electricity sale prices, in addition to reductions in operational and capital expenditure. Further improvements to the process, such as increased carbonate regeneration through intermediary steps, would have the potential to increase the profitability, by reducing purge-flow requirements and subsequent disposal costs, although they would include inherent costs.

The results of this project highlight the importance of maintaining particle activity and minimising waste flows on the overall economic potential of CaL processes. The findings presented demonstrate the potential of running CaL processes with purge and make-up flow rates to maintain the average particle activity within the system. The results indicated the potential of utilising solids storage for load shifting, with a comparison of its potential

economic benefit versus increased capture rates demonstrated in the second sensitivity analysis. Additionally, the trends identified within the report indicate the potential of improving system outputs by increasing cycle number, the model developed can be utilised to further substantiate this claim.

6. Future Work

This section details potential options for future work identified during the project to both improve the accuracy of gathered results and to build on the key findings of the project.

6.1. Process Modelling Future Work

During the modelling section of the project several key assumptions were made regarding reaction conditions which will have impacted on the accuracy of gathered results. Potential improvements that may be made to the model will be detailed in this section:

- Reaction kinetics were not considered within the reactor modelling for both the calciner and carbonator. Whilst Aspen+ is a steady state modelling software, some basic calculations could have been included within the reactors, beyond the basic stoichiometry assumptions made. In order to better integrate these assumptions, the RStoic reactor blocks used within the model should be replaced by r-CSTR reactor blocks to provide more accurate control of reaction conditions.
- The model does not consider the presence of SOx emissions within the FG This would result in a major impact upon the carbon capture capability of solid flows, as SOx emissions react with CaO. [85] This consideration should be integrated into the model by use of a pre-carbonator reactor block for SOx removal.
- Neither the process modelling or economic calculations review the impacts of detailed heat exchanger design. Developing a more accurate model of the heat exchangers used would provide a better representation of energy balances within the system.
- The model does not consider heat integration of the system with parallel process on the heat input or extraction side, the development of a fully integrated model would provide more accurate results for specific cases.
- The modelling of steam fluidisation within the calciner block is based on assumptions related to the particle activity [63], this does not provide an accurate model of the fluidisation agent flow required within the reactor to simulate fluidisation effects. Further calculations are required to provide accurate data on the required mass flows and parasitic load of steam generation.
- Aspen+ has been used to provide a steady-state process model, as a result the project does not include a simulation the interaction of particles throughout repeated cycling, therefore it can only provide information on system effects in the single cycle modelled. To provide a more detailed understanding of the behaviour of the calcium looping system over time a dynamic model should be developed.
- The impacts of steam on solids mechanics (including particle disintegration and attrition) have not been included in this project and are difficult to model using Aspen+, due to its steady-state operation. These effects would be better considered in a dynamic model. Additionally, the current consideration of steam impacts on particle activity is included solely as a multiplier, however, they could be more accurately modelled by the integration of an intermediary reaction block prior to the calciner, to model partial conversion to calcium hydroxide within the process.
- The impact of H_2O presence within the carbonator has been ignored due to conflicting evidence within the literature [89, 93, 94]
- Assumptions made surrounding average particle activity (X_{AVE}) could be improved by considering specific reactor design, including volumetric limitations and heat flows within the reactor.

6.2. Economic Modelling Future Work

- Accurate sizing of components including heat exchangers and reactors is key in the calculation of system capital expenditure, the sizing would be improved following the aforementioned improvements in process modelling.
- There are key operational expenditure considerations not included within this work, including internal solids conveying costs, which can be associated with energy requirement costs for moving a mass over the internal distances [111] and labour costs. The inclusion of these parameters would provide a more accurate economic model of the system.

Bibliography

[1] "Paris Agreement | Climate Action." https://ec.europa.eu/clima/policies/international/negotiations/paris_en (accessed Apr. 29, 2021).

[2] M. Victoria, K. Zhu, T. Brown, G. B. Andresen, and M. Greiner, "The role of storage technologies throughout the decarbonisation of the sector-coupled European energy system," *Energy Convers. Manag.*, vol. 201, Jun. 2019, doi: 10.1016/j.enconman.2019.111977.

[3] J. Jensen, "Introduction," in *Energy Storage*, Elsevier, 1980, pp. 1–4.

[4] A. J. Carrillo, D. P. Serrano, P. Pizarro, and J. M. Coronado, "Improving the thermochemical energy storage performance of the Mn2O3/Mn3O4 redox couple by the incorporation of iron," *ChemSusChem*, vol. 8, no. 11, pp. 1947–1954, Jun. 2015, doi: 10.1002/cssc.201500148.

[5] S. Vazquez, S. M. Lukic, E. Galvan, L. G. Franquelo, and J. M. Carrasco, "Energy storage systems for transport and grid applications," *IEEE Trans. Ind. Electron.*, vol. 57, no. 12, pp. 3881–3895, Dec. 2010, doi: 10.1109/TIE.2010.2076414.

[6] Y. Yan, K. Wang, P. T. Clough, and E. J. Anthony, "Developments in calcium/chemical looping and metal oxide redox cycles for high-temperature thermochemical energy storage: A review," *Fuel Processing Technology*, vol. 199. Elsevier B.V., p. 106280, Mar. 01, 2020, doi: 10.1016/j.fuproc.2019.106280.

[7] A. J. Carrillo, J. González-Aguilar, M. Romero, and J. M. Coronado, "Solar Energy on Demand: A Review on High Temperature Thermochemical Heat Storage Systems and Materials," *Chem. Rev.*, vol. 119, no. 7, pp. 4777–4816, Mar. 2019, doi: 10.1021/acs.chemrev.8b00315.

[8] "Thermochemical Energy Storage - an overview | ScienceDirect Topics." https://www.sciencedirect.com/topics/engineering/thermochemical-energy-storage (accessed May 02, 2021).

[9] "CCUS technology innovation – CCUS in Clean Energy Transitions – Analysis - IEA." https://www.iea.org/reports/ccus-in-clean-energy-transitions/ccus-technology-innovation (accessed Apr. 30, 2021).

[10] I. Energy Ageny, "Technology Roadmap Energy storage." Accessed: Apr. 30, 2021. [Online]. Available: www.iea.org.

[11] A. R. Dehghani-Sanij, E. Tharumalingam, M. B. Dusseault, and R. Fraser, "Study of energy storage systems and environmental challenges of batteries," *Renewable and Sustainable Energy Reviews*, vol. 104. Elsevier Ltd, pp. 192–208, Apr. 01, 2019, doi: 10.1016/j.rser.2019.01.023.

[12] "CARBON DIOXIDE CAPTURE AND STORAGE."

[13] M. Astolfi, E. De Lena, and M. C. Romano, "Improved flexibility and economics of Calcium Looping power plants by thermochemical energy storage," *Int. J. Greenh. Gas Control*, vol.

83, pp. 140–155, Apr. 2019, doi: 10.1016/j.ijggc.2019.01.023.

[14] N. Rodríguez, M. Alonso, and J. C. Abanades, “Average activity of CaO particles in a calcium looping system,” *Chem. Eng. J.*, vol. 156, no. 2, pp. 388–394, Jan. 2010, doi: 10.1016/j.cej.2009.10.055.

[15] J. C. Abanades, “The maximum capture efficiency of CO2 using a carbonation/calcination cycle of CaO/CaCO3,” *Chem. Eng. J.*, vol. 90, no. 3, pp. 303–306, Dec. 2002, doi: 10.1016/S1385-8947(02)00126-2.

[16] H. Dieter, A. R. Bidwe, G. Varela-Duelli, A. Charitos, C. Hawthorne, and G. Scheffknecht, “Development of the calcium looping CO2 capture technology from lab to pilot scale at IFK, University of Stuttgart,” *Fuel*, vol. 127, pp. 23–37, Jul. 2014, doi: 10.1016/j.fuel.2014.01.063.

[17] M. Helbig, J. Hilz, M. Haaf, A. Daikeler, J. Ströhle, and B. Epple, “Long-term Carbonate Looping Testing in a 1 MWth Pilot Plant with Hard Coal and Lignite,” in *Energy Procedia*, Jul. 2017, vol. 114, pp. 179–190, doi: 10.1016/j.egypro.2017.03.1160.

[18] B. Arias *et al.*, “Demonstration of steady state CO2 capture in a 1.7MWth calcium looping pilot,” *Int. J. Greenh. Gas Control*, vol. 18, pp. 237–245, Oct. 2013, doi: 10.1016/j.ijggc.2013.07.014.

[19] B. Arias, M. Alonso, and C. Abanades, “CO2 Capture by Calcium Looping at Relevant Conditions for Cement Plants: Experimental Testing in a 30 kWth Pilot Plant,” *Ind. & Eng. Chem. Res.*, vol. 56, no. 10, pp. 2634–2640, Mar. 2017, doi: 10.1021/acs.iecr.6b04617.

[20] “Socratces Project Competitive & Sustainable Concentrated Solar Plants.” https://socratces.eu/the-project/ (accessed May 02, 2021).

[21] A. Muto and T. Hansen, “Demonstration of High-Temperature Calcium-Based Thermochemical Energy Storage System for use with Concentrating Solar Power Facilities,” *Apollo Phase 2 - Final Technical Report*, 2019. https://www.osti.gov/servlets/purl/1523643/ (accessed May 02, 2021).

[22] F. Sattari, M. Tahmasebpoor, J. M. Valverde, C. Ortiz, and M. Mohammadpourfard, “Modelling of a fluidized bed carbonator reactor for post-combustion CO2 capture considering bed hydrodynamics and sorbent characteristics,” *Chem. Eng. J.*, vol. 406, p. 126762, Feb. 2021, doi: 10.1016/j.cej.2020.126762.

[23] I. Martínez, R. Murillo, G. Grasa, and J. C. Abanades, “Integration of a calcium looping system for CO 2 capture in an existing power plant.”

[24] J. Blamey, E. J. Anthony, J. Wang, and P. S. Fennell, “The calcium looping cycle for large-scale CO2 capture,” *Progress in Energy and Combustion Science*, vol. 36, no. 2. Pergamon, pp. 260–279, Apr. 01, 2010, doi: 10.1016/j.pecs.2009.10.001.

[25] J. Carlos Abanades, E. J. Anthony, J. Wang, and J. E. Oakey, “Fluidized Bed Combustion Systems Integrating CO2 Capture with CaO,” *Environ. Sci. & Technol.*, vol. 39, no. 8, pp. 2861–2866, Mar. 2005, doi: 10.1021/es0496221.

[26] S. Shahkarami, R. Azargohar, A. K. Dalai, and J. Soltan, “Breakthrough CO2 adsorption in bio-based activated carbons,” *J. Environ. Sci. (China)*, vol. 34, pp. 68–76, Aug. 2015, doi:

10.1016/j.jes.2015.03.008.

[27] D. Y. C. Leung, G. Caramanna, and M. M. Maroto-Valer, “An overview of current status of carbon dioxide capture and storage technologies,” *Renewable and Sustainable Energy Reviews*, vol. 39. Elsevier Ltd, pp. 426–443, Nov. 01, 2014, doi: 10.1016/j.rser.2014.07.093.

[28] “The Paris Agreement | UNFCCC.” https://unfccc.int/process-and-meetings/the-paris-agreement/the-paris-agreement (accessed May 02, 2021).

[29] “Bio-CCS.” https://www.etipbioenergy.eu/sustainability/bio-ccs (accessed May 02, 2021).

[30] “Chapter Climate Change 2014 Synthesis Report Summary for Policymakers Summary for Policymakers.”

[31] “Is carbon capture too expensive? – Analysis - IEA.” https://www.iea.org/commentaries/is-carbon-capture-too-expensive (accessed May 02, 2021).

[32] “CCS Roadmap Storage strategy,” 2012.

[33] “Carbon capture, utilisation and storage - Fuels & Technologies - IEA.” https://www.iea.org/fuels-and-technologies/carbon-capture-utilisation-and-storage (accessed May 02, 2021).

[34] “Oxyfuel Combustion - an overview | ScienceDirect Topics.” https://www.sciencedirect.com/topics/engineering/oxyfuel-combustion (accessed May 31, 2021).

[35] Y. Wang, L. Zhao, A. Otto, M. Robinius, and D. Stolten, “A Review of Post-combustion CO2 Capture Technologies from Coal-fired Power Plants,” in *Energy Procedia*, Jul. 2017, vol. 114, pp. 650–665, doi: 10.1016/j.egypro.2017.03.1209.

[36] M. Wang, A. Lawal, P. Stephenson, J. Sidders, C. Ramshaw, and H. Yeung, “Post-combustion CO 2 Capture with Chemical Absorption: A State-of-the-art Review.”

[37] M. Kárászová *et al.*, “Post-combustion carbon capture by membrane separation, Review,” *Separation and Purification Technology*, vol. 238. Elsevier B.V., p. 116448, May 01, 2020, doi: 10.1016/j.seppur.2019.116448.

[38] “Chemical Looping Combustion - an overview | ScienceDirect Topics.” https://www.sciencedirect.com/topics/engineering/chemical-looping-combustion (accessed May 03, 2021).

[39] “Chemical Looping Reforming - an overview | ScienceDirect Topics.” https://www.sciencedirect.com/topics/engineering/chemical-looping-reforming (accessed May 03, 2021).

[40] “Energy Storing Cryogenic Carbon Capture Final Executive Summary Wyoming Clean Coal Technologies) Project Sponsor: State of Wyoming CFDA Number: Non-Federal Project Title: Energy Storing Cryogenic Carbon Capture PI: Larry Baxter,” 2016.

[41] P. Markewitz *et al.*, “Worldwide innovations in the development of carbon capture technologies and the utilization of CO 2,” doi: 10.1039/c2ee03403d.

[42] A. Alshehri, R. Khalilpour, A. Abbas, and Z. Lai, “Membrane systems engineering for post-combustion carbon capture,” in *Energy Procedia*, Jan. 2013, vol. 37, pp. 976–985, doi: 10.1016/j.egypro.2013.05.193.

[43] M. Oschatz and M. Antonietti, “A search for selectivity to enable CO 2 capture with porous adsorbents,” *Energy Environ. Sci*, vol. 11, p. 57, 2018, doi: 10.1039/c7ee02110k.

[44] N. Rodríguez, M. Alonso, and J. C. Abanades, “EXPERIMENTAL INVESTIGATION OF A CIRCULATING FLUIDIZED BED REACTOR TO CAPTURE CO 2 WITH CaO.”

[45] R. T. Symonds, D. Y. Lu, V. Manovic, and E. J. Anthony, “Pilot-Scale Study of CO 2 Capture by CaO-Based Sorbents in the Presence of Steam and SO 2,” doi: 10.1021/ie2030129.

[46] I. Renewable Energy Agency, “Methodology background document: Development of a decarbonisation pathway for the global energy system to 2050 A country-by-country analysis for the G20 based on IRENA’s REmap and Renewable Energy Benefits programmes,” 2017. Accessed: May 03, 2021. [Online]. Available: www.irena.org.

[47] S. Görtz, “EN1510 Examensarbete för civilingenjörsexamen i Energiteknik Battery energy storage for intermittent renewable electricity production A review and demonstration of energy storage applications permitting higher penetration of renewables.”

[48] T. Bowen, I. Chernyakhovskiy, and P. Denholm, “Grid-Scale Battery Storage: Frequently Asked Questions.” Accessed: Jun. 01, 2021. [Online]. Available: www.greeningthegrid.org.

[49] H. Chen, T. N. Cong, W. Yang, C. Tan, Y. Li, and Y. Ding, “Progress in electrical energy storage system: A critical review,” *Progress in Natural Science*, vol. 19, no. 3. Science Press, pp. 291–312, 2009, doi: 10.1016/j.pnsc.2008.07.014.

[50] I. Renewable Energy Agency, *INNOVATION OUTLOOK THERMAL ENERGY STORAGE About IRENA*. 2020.

[51] M. Aneke and M. Wang, “Energy storage technologies and real life applications – A state of the art review,” *Applied Energy*, vol. 179. Elsevier Ltd, pp. 350–377, Oct. 01, 2016, doi: 10.1016/j.apenergy.2016.06.097.

[52] O. Siddiqui and I. Dincer, “Development of a sustainable energy system utilizing a new molten-salt based hybrid thermal energy storage and electrochemical energy conversion technique,” *Sustain. Energy Technol. Assessments*, vol. 42, p. 100866, Dec. 2020, doi: 10.1016/j.seta.2020.100866.

[53] S. H. Gage *et al.*, “Technical and economic feasibility of molten chloride salt thermal energy storage systems,” *Sol. Energy Mater. Sol. Cells*, vol. 226, p. 111099, Jul. 2021, doi: 10.1016/j.solmat.2021.111099.

[54] K. Pielichowska and K. Pielichowski, “Phase change materials for thermal energy storage,” *Progress in Materials Science*, vol. 65. Elsevier Ltd, pp. 67–123, Aug. 01, 2014, doi: 10.1016/j.pmatsci.2014.03.005.

[55] A. H. Abedin and M. A. Rosen, “A Critical Review of Thermochemical Energy Storage

Systems," 2011.

[56] S. Wu, C. Zhou, P. Tremain, E. Doroodchi, and B. Moghtaderi, "A phase change calcium looping thermochemical energy storage system based on CaCO3/CaO-CaCl2," *Energy Convers. Manag.*, vol. 227, p. 113503, Jan. 2021, doi: 10.1016/j.enconman.2020.113503.

[57] B. Satya Sekhar, P. Muthukumar, and R. Saikia, "Tests on a metal hydride based thermal energy storage system," in *International Journal of Hydrogen Energy*, Feb. 2012, vol. 37, no. 4, pp. 3818–3824, doi: 10.1016/j.ijhydene.2011.05.114.

[58] A. Reiser, B. Bogdanović, and K. Schlichte, "Application of Mg-based metal-hydrides as heat energy storage systems," *Int. J. Hydrogen Energy*, vol. 25, no. 5, pp. 425–430, May 2000, doi: 10.1016/S0360-3199(99)00057-9.

[59] T. Block and M. Schmücker, "Metal oxides for thermochemical energy storage: A comparison of several metal oxide systems," *Sol. Energy*, vol. 126, pp. 195–207, Mar. 2016, doi: 10.1016/j.solener.2015.12.032.

[60] E. AUKRUST and A. MUAN, "Phase Relations in the System Cobalt Oxide–Manganese Oxide in Air," *J. Am. Ceram. Soc.*, vol. 46, no. 10, pp. 511–511, 1963, doi: 10.1111/j.1151-2916.1963.tb13790.x.

[61] J. Yan, C. Y. Zhao, and Z. H. Pan, "The effect of CO2 on Ca(OH)2 and Mg(OH)2 thermochemical heat storage systems," *Energy*, vol. 124, pp. 114–123, Apr. 2017, doi: 10.1016/j.energy.2017.02.034.

[62] F. Schaube, A. Wörner, and R. Tamme, "High temperature thermochemical heat storage for concentrated solar power using gas-solid reactions," *J. Sol. Energy Eng. Trans. ASME*, vol. 133, no. 3, Aug. 2011, doi: 10.1115/1.4004245.

[63] S. Champagne, D. Y. Lu, A. Macchi, R. T. Symonds, and E. J. Anthony, "Influence of Steam Injection during Calcination on the Reactivity of CaO-Based Sorbent for Carbon Capture," 2012, doi: 10.1021/ie3012787.

[64] "1911 Encyclopædia Britannica/Carbonates - Wikisource, the free online library." https://en.wikisource.org/wiki/1911_Encyclopædia_Britannica/Carbonates (accessed May 06, 2021).

[65] K. Visscher and J. B. J. Veldhuis, "COMPARISON OF CANDIDATE MATERIALS FOR SEASONAL STORAGE OF SOLAR HEAT THROUGH DYNAMIC SIMULATION OF BUILDING AND RENEWABLE ENERGY SYSTEM." Accessed: May 06, 2021. [Online]. Available: www.ecn.nl.

[66] M. Ives, R. C. Mundy, P. S. Fennell, J. F. Davidson, J. S. Dennis, and A. N. Hayhurst, "Comparison of Different Natural Sorbents for Removing CO2 from Combustion Gases, as Studied in a Bench-Scale Fluidized Bed," *Energy & Fuels*, vol. 22, no. 6, pp. 3852–3857, Sep. 2008, doi: 10.1021/ef800417v.

[67] T. D. Humphries *et al.*, "Dolomite: a low cost thermochemical energy storage material †," 2019, doi: 10.1039/c8ta07254j.

[68] Y. Ding and S. B. Riffat, "Thermochemical energy storage technologies for building applications: a state-of-the-art review," *Int. J. Low-Carbon Technol.*, vol. 8, no. 2, pp. 106–

116, Jun. 2013, doi: 10.1093/ijlct/cts004.

[69] P. Ammendola, F. Raganati, F. Miccio, A. N. Murri, and E. Landi, “Insights into utilization of strontium carbonate for thermochemical energy storage,” *Renew. Energy*, vol. 157, pp. 769–781, Sep. 2020, doi: 10.1016/j.renene.2020.05.048.

[70] A. Perejón, J. Miranda-Pizarro, L. A. Pérez-Maqueda, and J. M. Valverde, “On the relevant role of solids residence time on their CO 2 capture performance in the Calcium Looping technology On the relevant role of solids residence time on their CO 2 capture performance in the Calcium Looping technology On the relevant role of solids residence time on their CO 2 capture performance in the Calcium Looping technology.”

[71] “Process Modelling of the Calcium Looping Process and Validation Against 1 MWth Pilot Testing | Elsevier Enhanced Reader.” https://reader.elsevier.com/reader/sd/pii/S1876610217313322?token=3ED46C6698DE2F863086023EB33BDEAF50D591734866553A3EADEF801046F8C1261C9D1F9B8592C14FE5B77D2B7B5DF5&originRegion=eu-west-1&originCreation=20210507091107 (accessed May 07, 2021).

[72] C. Ortiz, R. Chacartegui, J. M. Valverde, J. A. Becerra, and L. A. Perez-Maqueda, “A new model of the carbonator reactor in the calcium looping technology for post-combustion CO2 capture,” *Fuel*, vol. 160, pp. 328–338, Aug. 2015, doi: 10.1016/j.fuel.2015.07.095.

[73] J.-P. Tranier, R. Dubettier, A. Darde, and N. Perrin, “Energy Procedia Air Separation, flue gas compression and purification units for oxy-coal combustion systems,” *Energy Procedia*, vol. 4, pp. 966–971, 2011, doi: 10.1016/j.egypro.2011.01.143.

[74] T. Shimizu, T. Hirama, H. Hosoda, K. Kitano, M. Inagaki, and K. Tejima, “A twin fluid-bed reactor for removal of CO2 from combustion processes,” *Chem. Eng. Res. Des.*, vol. 77, no. 1, pp. 62–68, 1999, doi: 10.1205/026387699525882.

[75] G. S. Grasa and J. Carlos Abanades, “CO2 Capture Capacity of CaO in Long Series of Carbonation/Calcination Cycles,” *Ind. & Eng. Chem. Res.*, vol. 45, no. 26, pp. 8846–8851, Nov. 2006, doi: 10.1021/ie0606946.

[76] M. Kavosh, K. Patchigolla, J. E. Oakey, E. J. Anthony, S. Champagne, and R. Hughes, “Pressurised calcination-atmospheric carbonation of limestone for cyclic CO2 capture from flue gases,” *Chem. Eng. Res. Des.*, vol. 102, pp. 116–123, Oct. 2015, doi: 10.1016/j.cherd.2015.06.024.

[77] G. S. Grasa, J. C. Abanades, M. Alonso, and B. González, “Reactivity of highly cycled particles of CaO in a carbonation/calcination loop,” *Chem. Eng. J.*, vol. 137, no. 3, pp. 561–567, Apr. 2008, doi: 10.1016/j.cej.2007.05.017.

[78] M. Erans, V. Manovic, and E. J. Anthony, “Calcium looping sorbents for CO 2 capture,” *Appl. Energy*, vol. 180, pp. 722–742, 2016, doi: 10.1016/j.apenergy.2016.07.074.

[79] A. Charitos *et al.*, “Experimental Validation of the Calcium Looping CO2 Capture Process with Two Circulating Fluidized Bed Carbonator Reactors,” *Ind. & Eng. Chem. Res.*, vol. 50, no. 16, pp. 9685–9695, Jul. 2011, doi: 10.1021/ie200579f.

[80] V. Manovic and E. J. Anthony, “Lime-Based Sorbents for High-Temperature CO 2 Capture-A

Review of Sorbent Modification Methods," *OPEN ACCESS Int. J. Environ. Res. Public Heal.*, vol. 7, p. 7, 2010, doi: 10.3390/ijerph7083129.

[81] J. C. Abanades, E. S. Rubin, and E. J. Anthony, "Sorbent Cost and Performance in CO2 Capture Systems," *Ind. & Eng. Chem. Res.*, vol. 43, no. 13, pp. 3462–3466, May 2004, doi: 10.1021/ie049962v.

[82] J. Ylätalo, J. Ritvanen, T. Tynjälä, and T. Hyppänen, "Model based scale-up study of the calcium looping process," *Fuel*, vol. 115, pp. 329–337, Jan. 2014, doi: 10.1016/j.fuel.2013.07.036.

[83] J. Ströhle, M. Junk, J. Kremer, A. Galloy, and B. Epple, "Carbonate looping experiments in a 1 MWth pilot plant and model validation," *Fuel*, vol. 127, pp. 13–22, Jul. 2014, doi: 10.1016/j.fuel.2013.12.043.

[84] C. K. Jayarathna, A. Mathisen, L. E. Øi, and L.-A. Tokheim, "Process Simulation of Calcium Looping with Indirect Calciner Heat Transfer," doi: 10.3384/ecp1511971.

[85] A. Coppola, F. Montagnaro, F. Scala, and P. Salatino, "Impact fragmentation of limestone-based sorbents for calcium looping: The effect of steam and sulphur dioxide," *Fuel Process. Technol.*, vol. 208, p. 106499, Nov. 2020, doi: 10.1016/j.fuproc.2020.106499.

[86] R. H. Borgwardt, "Calcium oxide sintering in atmospheres containing water and carbon dioxide," *Ind. & Eng. Chem. Res.*, vol. 28, no. 4, pp. 493–500, May 2002, doi: 10.1021/ie00088a019.

[87] S. Champagne, D. Y. Lu, A. Macchi, R. T. Symonds, and E. J. Anthony, "Influence of Steam Injection during Calcination on the Reactivity of CaO-Based Sorbent for Carbon Capture," *Ind. & Eng. Chem. Res.*, vol. 52, no. 6, pp. 2241–2246, Feb. 2013, doi: 10.1021/ie3012787.

[88] F. Donat, N. H. Florin, E. J. Anthony, and P. S. Fennell, "Influence of High-Temperature Steam on the Reactivity of CaO Sorbent for CO2 Capture," *Environ. Sci. & Technol.*, vol. 46, no. 2, pp. 1262–1269, Jan. 2012, doi: 10.1021/es202679w.

[89] V. Manovic, E. J. Anthony, and D. Y. Lu, "Sulphation and carbonation properties of hydrated sorbents from a fluidized bed CO2 looping cycle reactor," *Fuel*, vol. 87, no. 13–14, pp. 2923–2931, Oct. 2008, doi: 10.1016/j.fuel.2008.04.023.

[90] M. Hornberger, J. Moreno, M. Schmid, and G. Scheffknecht, "Experimental investigation of the calcination reactor in a tail-end calcium looping configuration for CO2 capture from cement plants," *Fuel*, vol. 284, p. 118927, Jan. 2021, doi: 10.1016/j.fuel.2020.118927.

[91] C. W. Bale *et al.*, "FactSage thermochemical software and databases," *Calphad Comput. Coupling Phase Diagrams Thermochem.*, vol. 26, no. 2, pp. 189–228, Jun. 2002, doi: 10.1016/S0364-5916(02)00035-4.

[92] A. Ebneyamini, Z. J. Li, J. Y. Kim, J. R. Grace, C. J. Lim, and N. Ellis, "Effect of calcination temperature and extent on the multi-cycle CO2 carrying capacity of lime-based sorbents," *J. CO2 Util.*, vol. 49, p. 101546, Jul. 2021, doi: 10.1016/j.jcou.2021.101546.

[93] B. Dou, Y. Song, Y. Liu, and C. Feng, "High temperature CO2 capture using calcium oxide sorbent in a fixed-bed reactor | Elsevier Enhanced Reader."

https://reader.elsevier.com/reader/sd/pii/S0304389410009763?token=FB660C85C4994DFAE6BB74310E4A49C227229AFDE59A91BDD6018E0FAE060C4B61F82068009AA0D479D73C6D98945F43&originRegion=eu-west-1&originCreation=20210607090552 (accessed Jun. 07, 2021).

[94] B. Arias, G. Grasa, J. C. Abanades, V. Manovic, and E. J. Anthony, "The Effect of Steam on the Fast Carbonation Reaction Rates of CaO," *Ind. & Eng. Chem. Res.*, vol. 51, no. 5, pp. 2478–2482, Jan. 2012, doi: 10.1021/ie202648p.

[95] M. Bailera, S. Pascual, P. Lisbona, and L. M. Romeo, "Modelling calcium looping at industrial scale for energy storage in concentrating solar power plants," *Energy*, vol. 225, p. 120306, Jun. 2021, doi: 10.1016/j.energy.2021.120306.

[96] "Two-Phase Flow Heat Exchangers Thermal-Hydraulic Fundamentals and Design."

[97] D. W. Green and R. H. Perry, "HEAT EXCHANGERS FOR SOLIDS," 2008, Accessed: May 20, 2021. [Online]. Available: https://www.accessengineeringlibrary.com/content/book/9780071422949/toc-chapter/chapter11/section/section51.

[98] G. S. Grasa, J. C. Abanades, M. Alonso, and B. González, "Reactivity of highly cycled particles of CaO in a carbonation/calcination loop," *Chem. Eng. J.*, vol. 137, no. 3, pp. 561–567, Apr. 2008, doi: 10.1016/j.cej.2007.05.017.

[99] S. Begum, M. G. Rasul, D. Akbar, and D. Cork, "An experimental and numerical investigation of fluidized bed gasification of solid waste," *Energies*, vol. 7, no. 1, pp. 43–61, Dec. 2014, doi: 10.3390/en7010043.

[100] "Flue Gas - an overview | ScienceDirect Topics." https://www.sciencedirect.com/topics/chemistry/flue-gas (accessed Jun. 03, 2021).

[101] H. Noh, K. Kang, C. Huh, S. Kang, and S. J. Han, "Conceptualization of CO2 Terminal for Offshore CCS Using System Engineering Process," no. 2, 2019.

[102] S. Wu, C. Zhou, E. Doroodchi, and B. Moghtaderi, "A unique phase change redox cycle using CuO/Cu2O for utility-scale energy storage," *Energy Convers. Manag.*, vol. 188, pp. 366–380, May 2019, doi: 10.1016/j.enconman.2019.03.055.

[103] I. Martínez, G. Grasa, R. Murillo, B. Arias, and J. C. Abanades, "Kinetics of Calcination of Partially Carbonated Particles in a Ca-Looping System for CO2 Capture," *Energy & Fuels*, vol. 26, no. 2, pp. 1432–1440, Jan. 2012, doi: 10.1021/ef201525k.

[104] A. Technology, "Aspen Physical Property Methods," 2013. Accessed: Jun. 07, 2021. [Online]. Available: http://www.aspentech.com.

[105] G. S. Grasa and J. C. Abanades, "CO2 capture capacity of CaO in long series of carbonation/calcination cycles," *Ind. Eng. Chem. Res.*, vol. 45, no. 26, pp. 8846–8851, Dec. 2006, doi: 10.1021/ie0606946.

[106] G. Grasa, J. C. Abanades, and E. J. Anthony, "Effect of partial carbonation on the cyclic CaO carbonation reaction," *Ind. Eng. Chem. Res.*, vol. 48, no. 20, pp. 9090–9096, Oct. 2009, doi: 10.1021/ie900443y.

[107] A. Silaban and D. P. Harrison, “High temperature capture of carbon dioxide: Characteristics of the reversible reaction between cao(s) and co2(g),” *Chem. Eng. Commun.*, vol. 137, no. 1, pp. 177–190, Jun. 1995, doi: 10.1080/00986449508936375.

[108] N. Rodríguez, M. Alonso, and J. C. Abanades, “Average activity of CaO particles in a calcium looping system,” *Chem. Eng. J.*, vol. 156, pp. 388–394, 2010, doi: 10.1016/j.cej.2009.10.055.

[109] G. M. Castilla, D. C. Guío-pérez, S. Papadokonstantakis, and D. Pallarès, “Techno-economic assessment of calcium looping for thermochemical energy storage with CO 2 capture,” pp. 1–18, 2021.

[110] “1 EUR to USD | Convert Euros to US Dollars | Xe.” https://www.xe.com/currencyconverter/convert/?Amount=1&From=EUR&To=USD (accessed May 24, 2021).

[111] A. Alovisio, R. Chacartegui, C. Ortiz, J. M. Valverde, and V. Verda, “Optimizing the CSP-Calcium Looping integration for Thermochemical Energy Storage 1.”

Appendix A – Process Model with Heaters for Heat Integration

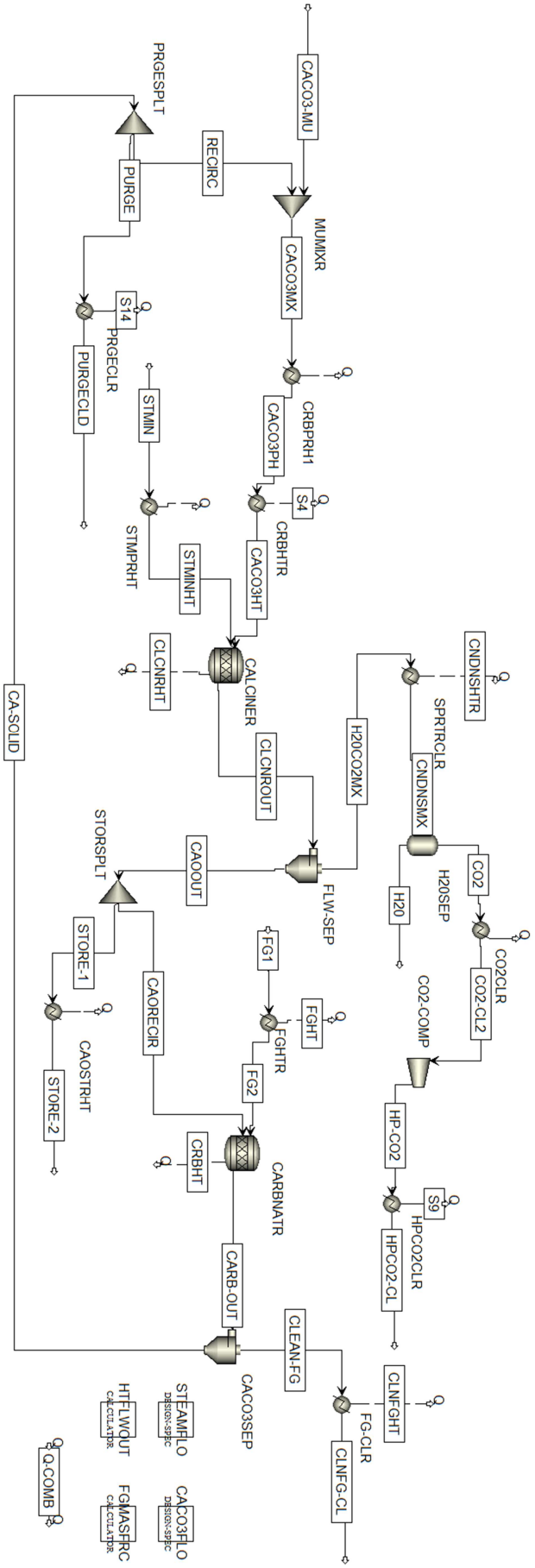

Appendix B – Calcium Looping ASPEN+ Model Inputs

Table 5 - Reactor Inputs

Block Name	Block Type	Input	
		Variable	Value
CALCINER	RStoic	Temperature (K)	925
		Pressure (atm)	1
		Reaction Stoichiometry	CACO3(CIPSD) --> CAO(CIPSD) + CO2(MIXED)
		Fractional Conversion (CACO3 (CIPSD))	0.95
CARBNTR	RStoic	Temperature (K)	650
		Pressure (atm)	1
		Reaction Stoichiometry	CAO(CIPSD) + CO2 --> CACO3(CIPSD)
		Fractional Conversion (CAO (CIPSD))	0.7

Table 6 - Splitter and Mixer Inputs

Block Name	Block Type	Input	
		Variable	Value
FLW-SEP	Cyclone	Model	Cyclone
		Mode	Design
		Calculation Method	Muschelknautz
		Type	Stairmand-HE
		Wall Friction Coefficient	0,0075
		Constant D	3
		Constant Kg	0,025
		Design Pressure Drop	0,01
		Number of Cyclones	1
		Max Iterations	30
		Error Tolerance	0,0001
STORSPLT	FSplit	Split Fraction (CAORECIRC)	0,999
H2OSEP	Flash2	Temperature (K)	293
		Pressure (atm)	1
		Valid Phases	Vapor-Liquid-Liquid
CACO3SEP	Cyclone	Model	Cyclone
		Mode	Design
		Calculation Method	Muschelknautz
		Type	Stairmand-HE
		Wall Friction Coefficient	0,0075
		Constant D	3
		Constant Kg	0,025

		Design Pressure Drop	0,01
		Number of Cyclones	1
		Max Iterations	30
		Error Tolerance	0,0001
PRGESPLT	FSplit	Flow (kmol/s)	*adjusted by calculator block HTFLWOUT
MUMIXR	Mixer	Pressure (atm)	1
		Max Iterations	30
		Error Tolerance	0,0001

Table 7 - Compressor Inputs

Block Name	Block Type	Input	
		Variable	Value
CO2-COMP	Compr	Type	Isentropic
		Discharge Pressure (kPa)	1600
		Isentropic	0,9
		Mechanical	0,98

Table 8 - Heater Inputs

Block Name	Block Type	Input	
		Variable	Value
CRBHTR	Heater	Temperature (°C)	950
		Pressure (atm)	1
STMPRHT	Heater	Temperature (°C)	950
		Pressure (atm)	1
PRGECLR	Heater	Temperature (°C)	30
		Pressure (atm)	1
SPRTRCLR	Heater	Temperature (°C)	20
		Pressure (atm)	1
CO2CLR	Heater	Temperature (°C)	20
		Pressure (atm)	1
HPCO2CLR	Heater	Temperature (°C)	-17
		Pressure (atm)	16
FGCLR	Heater	Temperature (°C)	100
		Pressure (atm)	1
FGHTR	Heater	Temperature (°C)	650
		Pressure (atm)	1
CRBCLR	Heater	Temperature (°C)	650
		Pressure (atm)	1
CAOSTRHTR	Heater	Temperature (°C)	30
		Pressure (atm)	1

Table 9 – Design-Spec Blocks

Block Name	Block Type	Input		
		Tab	Variable	Input

STEAMFLO	DESIGN-SPEC	Define	STEAMIN	Mass-Flow Stream=STMIN Substream=MIXED Component=WATER Units=kg/hr
			CO2OUT	Mass-Flow Stream=STMIN Substream=MIXED Component=WATER Units=kg/hr
		Spec	SPEC	STEAMIN/CO2OUT
			Target	0,4
			Tolerance	0,001
		Vary	Manipulated Variable	Mass-Flow Stream=STMIN Substream=MIXED Component=WATER Units=kg/hr
			Manipulated Variable Limits	Lower =1000 Upper = 1000000
FGFLO	DESIGN-SPEC	Define	CO2OUT	Mole-Flow Stream=CLEAN-FG Substream=MIXED Component=CO2 Units=kmol/hr
			CO2IN	Mole-Flow Stream=FG1 Substream=MIXED Component=CO2 Units=kmol/hr
		Spec	SPEC	CO2OUT/CO2IN
			Target	0,9
			Tolerance	0,0001
		Vary	Manipulated Variable	Mole-Flow Stream=FG1 Substream=MIXED Component=CO2 Units=kmol/hr
			Manipulated Variable Limits	Lower =1000 Upper =100000

Table 10 - Calculator Blocks

Block Name	Block Type	Input		
			Name	Definition
HTFLWOUT	CALCULATOR	Import Variables	CLCNRHT	Heat-Duty Stream=CLCNRHT Units=kW
			CRBNTRHT	Heat-Duty Stream=CRBHT Units=kW
			STMPRHT	Heat-Duty Stream=S3 Units=kW
			CACO3HT1	Heat-Duty Stream=S6 Units=kW
			CACO3HT2	Heat-Duty Stream=S4 Units=kW
			H2OSEP	Heat-Duty Stream=CNDNSHTR Units=kW

			CO2CL	Heat-Duty Stream=S13 Units=kW
			CMPCO2CL	Heat-Duty Stream=S9 Units=kW
			FGPRHT	Heat-Duty Stream=FGHT Units=kW
			FGOUTCLR	Heat-Duty Stream=CLNFGHT Units=Kw
			CAOSTRCL	Heat-Duty Stream=S11 Units=kW
			PRGECLR	Heat-Duty Stream=S14 Units=kW
			CAOSTR	Mole-Flow Stream=STORE-1 Substream=CIPSD Component=CAO Units=kmol/sec
			CACO3STR	Mole-Flow Stream=STORE-1 Substream=CIPSD Component=CACO3 Units=kmol/sec
			CACO3LST	Mole-Flow Stream=CLEAN-FG Substream=CIPSD Component=CACO3 Units=kmol/sec
			FGMASSFL	Mole-Flow Stream=FG1 Substream=MIXED Component=CO2 Units=kmol/sec
			CAOFLW	Mole-Flow Stream=CAORECIR Substream=CIPSD Component=CAO Units=kmol/sec
		Export Variables	COMBINED	Heat-Duty Stream=Q-COMB Units=kW
			MAKEUPFL	Mole-Flow Stream=CACO3-MU Substream=CIPSD Component=CACO3 Units=kmol/sec
			RECIRCFL	Mole-Flow Stream=CACO3MX Substream=CIPSD Component=CACO3 Units=kmol/sec
FGMASFRC	CALCULATOR	Import Variables	CO2	Mass-Flow Stream=FG1 Substream=MIXED Component=CO2 Units=kg/hr
		Export Variables	N2	Mass-Flow Stream=FG1 Substream=MIXED Component=N2 Units=kg/hr

			H20	Mass-Flow Stream=FG1 Substream=MIXED Component=WATER Units=kg/hr
			O2	Mass-Flow Stream=FG1 Substream=MIXED Component=O2 Units=kg/hr

Appendix C – Detailed Results Base Case

Table 11 - Base Case CaCO3 Flow Rates

Simulation	Target Power (MW)	Target Activity	CC Rate	Cycle Number	Internal Flow Rate (kmol/s)	CaCO3 Mass Flow Rate (tonne/hr)	Make Up Flow (kmol/sec)	Make Up Flow (tonne/hr)	Purge Flow (kmol/s)
1	100	0,7	0,95	1	0,620	223,4	0,620	223,3	0,618
2	200	0,7	0,95	1	1,240	446,7	1,240	446,8	1,235
3	300	0,7	0,95	1	1,860	670,2	1,860	670,2	1,853
4	400	0,7	0,95	1	2,462	886,9	2,462	886,9	2,452
5	500	0,7	0,95	1	3,087	1112,2	3,087	1112,2	3,075
6	600	0,7	0,95	1	3,720	1340,4	3,720	1340,4	3,706
7	700	0,7	0,95	1	4,340	1563,7	4,340	1563,8	4,323
8	800	0,7	0,95	1	4,960	1787,7	4,960	1787,2	4,941
9	900	0,7	0,95	1	5,580	2010,6	5,580	2010,6	5,558
10	1000	0,7	0,95	1	6,200	2234	6,200	2233,9	6,176

Simulation	Target Power (MW)	Target Activity	CC Rate	Cycle Number	Disposal Cost ($/annum)	Reactor Loading Cost annualised ($/annum)	Material OPEX ($/annum)
1	100	0,7	0,95	1	19500000	9,308158027	37437485,57
2	200	0,7	0,95	1	39100000	18,61631605	74874965,83
3	300	0,7	0,95	1	58600000	27,92447408	112312456,6
4	400	0,7	0,95	1	77600000	36,95653735	148639487
5	500	0,7	0,95	1	97400000	46,3421914	186388662,2
6	600	0,7	0,95	1	117400000	55,8489556	224624943,3
7	700	0,7	0,95	1	136900000	65,15711237	262062423,8
8	800	0,7	0,95	1	156000000	74,46526913	299499904,3
9	900	0,7	0,95	1	176000000	83,7734259	336937384,8
10	1000	0,7	0,95	1	196000000	93,08158266	374374865,3

Simulation	Target Power (MW)	Target Activity	CC Rate	Cycle Number	True Calciner Power (kW)	Carbonator Power (kW)	Calciner Cost (M$)	Carbonator Cost (M$)	Reactor Costs (M$/annum)
1	100	0,7	0,95	1	-100001	71884,32	73,7	78,9	7,63
2	200	0,7	0,95	1	-200001	143766	117,2	125,6	12,1
3	300	0,7	0,95	1	-300002	215645,2	153,9	164,5	15,9
4	400	0,7	0,95	1	-397036	285390,2	185,7	198,8	19,2
5	500	0,7	0,95	1	-497870	357863,2	216,1	231,3	22,4
6	600	0,7	0,95	1	-600004	431268,8	244,9	262,1	25,4
7	700	0,7	0,95	1	-700004	503138,6	271,5	290,7	28,1
8	800	0,7	0,95	1	-800005	575006,1	296,9	317,9	30,7
9	900	0,7	0,95	1	-900006	646871,2	321,3	344	33,3
10	1000	0,7	0,95	1	-1000006	718734	344,8	370	35,7

Simulation	Target Power (MW)	Target Activity	CC Rate	Cycle Number	True Calciner Power (kW)	Carbonator Power (kW)	Calciner Cost (M$)	Carbonator Cost (M$)	Reactor Costs (M$/annum)
1	100	0,7	0,95	1	-100001	71884,32	73,7	78,9	7,6
2	200	0,7	0,95	1	-200001	143766	117,2	125,5	12,1
3	300	0,7	0,95	1	-300002	215645,2	153,9	164,8	15,9
4	400	0,7	0,95	1	-397036	285390,2	185,7	198,8	19,2
5	500	0,7	0,95	1	-497870	357863,2	216	231,4	22,3
6	600	0,7	0,95	1	-600004	431268,8	244,8	262,2	25,3
7	700	0,7	0,95	1	-700004	503138,6	271,5	290,7	28,1
8	800	0,7	0,95	1	-800005	575006,1	296,9	317,9	30,7
9	900	0,7	0,95	1	-900006	646871,2	321,3	344	33,2
10	1000	0,7	0,95	1	-1000006	718734	344,8	369,1	35,7

DEPARTMENT OF SPACE EARTH AND ENVIRONMENT
CHALMERS UNIVERSITY OF TECHNOLOGY
Gothenburg, Sweden 2021
www.chalmers.se

CHALMERS
UNIVERSITY OF TECHNOLOGY